Chemical aspects of metal ion chelation in the synthesis and application antibody-based radiotracers

Boros, Eszter ; Holland, Jason P

Abstract: Radiometals are becoming increasingly accessible and are utilized frequently in the design of radiotracers for imaging and therapy. Nuclear properties ranging from the emission of -rays and +-particles (imaging) to Auger electron and − and -particles (therapy) in combination with long half-lives are ideally matched with the relatively long biological half-life of monoclonal antibodies in vivo. Radiometal labeling of antibodies requires the incorporation of a metal chelate onto the monoclonal antibody. This chelate must coordinate the metal under mild conditions required for the handling of antibodies, as well as provide high kinetic, thermodynamic, and metabolic stability once the metal ion is coordinated to prevent release of the radionuclide before the target site is reached in vivo. Herein, we review the role of different radiometals that have found applications of the design of radiolabeled antibodies for imaging and radioimmunotherapy. Each radionuclide is described regarding its nuclear synthesis, coordinative preference, and radiolabeling properties with commonly used and novel chelates, as well as examples of their preclinical and clinical applications. An overview of recent trends in antibody-based radiopharmaceuticals is provided to spur continued development of the chemistry and application of radiometals for imaging and therapy.

DOI: https://doi.org/10.1002/jlcr.3590

Chemical aspects of metal ion chelation in the synthesis and application antibody-based radiotracers

Eszter Boros[1]* and Jason P. Holland[2]*

[1] Stony Brook University, Department of Chemistry, 100 Nicolls road, 11790 Stony Brook, NY, United States

[2] University of Zurich, Department of Chemistry, Winterthurerstrasse 190, CH-8057 Zurich, Switzerland

*** Correspondence:**

Eszter Boros

Tel: +1.631.632.8572

E-mail: eszter.boros@stonybrook.edu

Jason P. Holland

Tel: +41.44.63.53990

E-mail: jason.holland@chem.uzh.ch

Running Title: *Metal coordination chemistry for radiolabelling antibodies*

Word count (Main text):

Abstract

Radiometals are becoming increasingly accessible and are utilized frequently in the design of radiotracers for imaging and therapy. Nuclear properties ranging from the emission of γ-ray and β^+-particles (imaging) to Auger electron, β^- and α-particles (therapy) in combination with long half-lives are ideally matched with the relatively long biological half-life of monoclonal antibodies *in vivo*. Radiometal labelling of antibodies requires the incorporation of a metal chelate onto the monoclonal antibody. This chelate must coordinate the metal under mild conditions required for the handling of antibodies, as well as provide high kinetic, thermodynamic and metabolic stability once the metal ion is coordinated in order to prevent *in vivo* release of the radionuclide before the target site is reached. Herein, we review the role of different radiometals that have found applications the design of radiolabelled antibodies for imaging and radioimmunotherapy. Each radionuclide is described with regard to its nuclear synthesis, coordinative preference, and radiolabelling properties with commonly used chelates. A summary of recent developments in the area of chelate synthesis, as well as examples of their preclinical and clinical applications is presented. The aims of review are to provide an overview of recent trends in antibody-based radiopharmaceuticals and to spur continued development of the chemistry and application of radiometals for imaging and therapy.

Key words

Radiometals, chelates, coordination chemistry, immuno-PET, radioimmunotherapy

Introduction

In the pharmaceutical industry, biological products (biologics) and related biosimilar compounds represent one of the fastest growth sectors. In 2016, the size of the biologics market was estimated to be ~$200 billion USD. Recent forecasts predict continued growth at around 10% per annum with the market reaching ~$480 billion USD by 2024. Biologics include recombinant hormones and proteins, as well as cellular- and gene-based therapies, but the majority of this growth is driven by new vaccines and monoclonal antibodies (mAbs). Monoclonal antibodies or antibody-drug conjugates (ADCs) represent the single most important branch of biologics.[1] Between 2011 and August 2017, the United States Federal Drug Administration (US-FDA) approved a total of 235 New Molecular Entities (NMEs), of which 37 were either mAbs or ADCs for therapy (Figure 1). This growing trend is supported by historical data which suggest that biologics, and mAbs in particular, have received higher approval rates than conventional small-molecule drugs.[2] With prescription costs for mAb-based treatments estimated to be around 22-times more than small-molecule therapies, and profit margins often over 40%, it is easy to see the commercial attraction of biologics. However, this success is partially offset by the longer time frames required from initial clinical trials to full approval, more stringent manufacturing regulations, and the associated increase in costs. Recent changes to US legislation, implemented as part of the Patient Protection and Affordable Care Act of 2010, are also helping to create an abbreviated licensure pathway for NMEs that are demonstrated to be “biosimilar” to, or “interchangeable” with, an FDA-licensed biological product. This new legal framework will speed-up the discovery and clinical translation of mAb-based agents.

In nuclear medicine, desirable biochemical properties including high target affinity, specificity and selectivity, pre-optimised pharmacokinetics, and relative ease of selection using

various library technologies mean that antibody-based radiotracers are attractive platforms for developing diagnostic imaging and radioimmunotherapy (RIT) agents.[3–6] Nevertheless, production and validation of radiolabelled mAbs for use as immuno-single photon emission computed tomography (immuno-SPECT), immuno-positron emission tomography (immuno-PET) or RIT agents is non-trivial.[3] Synthesis of radiolabelled mAbs requires chemical reactions on the protein (Figure 2). Functionalisation usually involves post-translational modification of amino-acid side chains (particularly peptide bond formation using the primary amine group of lysine residues), derivatisation of cysteine sulfhydryl groups, or site-specific labelling of glycans using chemical and/or enzymatic methods.[7,8] More recent protein engineering routes have also exploited site-specific enzymatic ligation with prominent methods including transglutaminase derivatisation, sortase coupling and formylglycine reactions to produce a range of ADCs.[7–9] While the chemical nature of the linker group plays an important role in determining the metabolic stability and pharmacokinetics of a radiolabelled mAb, an equally important decision revolves around the choice of the radiometal ion and the chelation chemistry used to produce thermodynamically and kinetically stable radiometal ion complexes.[10] In this review, we discuss the chemical requirements for chelation of various radiometal ions and highlight selected applications of radiometal chemistry in the development of radiotracers for immuno-PET, immune-SPECT and RIT.[11]

1. Radionuclides for antibody imaging and therapy

In this issue of the Journal of Labelled Compounds and Radiopharmaceuticals, Engle and co-workers present an overview of the emerging radionuclides for use in combination with mAbs for diagnostic and RIT applications. Pertinent physical decay characteristics of 11 radiometal ions, and for comparison three different iodine radionuclides are presented in Table 1.[12] When selecting

a radionuclide for labelling antibodies or antibody-related constructs, the most crucial decision is to ensure that the physical half-life of the radionuclide is a reasonable match to the expected biological half-life of the radiotracer *in vivo*.[10] For example, ^{68}Ga ($t_{1/2}$ = 67.7 min.) is an excellent radionuclide for producing PET radiotracers based on small-molecules and peptides but would be an inappropriate choice for developing immuno-PET radiotracers based on full-sized mAbs (molecular weight ~150 kDa). Experience has found that mAbs reach optimum target (usually tumour) uptake and present maximal tumour-to-background contrast ratios in mouse models at around 24 – 96 h post-administration. Hence, in this pharmacokinetic situation, ^{68}Ga is likely to undergo complete decay before the biodistribution of a radiolabelled mAb reaches the optimum imaging window. Notably, in humans the pharmacokinetic profiles of radiolabelled mAbs are often slower than in rodents, with optimum target accumulation and image contrast achieved at time points beyond 72 h post-administration of the radiotracer. Such prolonged circulation times necessitate the use of radionuclides that have physical half-lives ranging from ca. 10 hours to several days. For immuno-PET imaging, ^{64}Cu, ^{86}Y, ^{89}Zr and ^{124}I are the most commonly used radionuclides, whereas for immuno-SPECT, ^{67}Ga, ^{99m}Tc, ^{111}In, ^{123}I and ^{177}Lu have been the radionuclides of choice. The majority of radiolabelled mAbs for applications in RIT use the beta-emitting radionuclides ^{90}Y, ^{131}I, and ^{177}Lu. Other radionuclides of note for potential RIT applications include the dual-decay mode of ^{64}Cu (branching ratio of 38.5% beta-decay to the daughter nuclide ^{65}Zn), ^{67}Cu[13] and the alpha emitter ^{225}Ac.[14,15]

2. **Copper radiolabelled antibodies**

Copper has a range of radionuclides with varying decay characteristics that are suitable for applications in both nuclear imaging and molecularly targeted radionuclide therapy.[16] PET

imaging radionuclides of copper include ^{60}Cu ($t_{1/2}$ = 23.7 min.), ^{61}Cu ($t_{1/2}$ = 3.333 h), ^{62}Cu ($t_{1/2}$ = 9.67 min.) but with the possible exception of ^{61}Cu for use in radiolabelling small peptides, proteins and antibody-based fragments, the most suitable radionuclide for combination with immuno-PET is ^{64}Cu.[17] In addition to PET imaging, ^{64}Cu also shows potential for therapeutic applications via separate decay involving beta-particle emission. However, ^{67}Cu ($t_{1/2}$ = 61.83 h; β– = 100%) with a maximum linear energy transfer of 561.7 keV is one of the most promising radionuclides for potential development of ^{67}Cu-mAbs for RIT.[18]

While the radiochemical landscape of copper radionuclides presents opportunities for developing imaging and therapeutic agents, controlling the chemistry of copper ions *in vivo* remains a formidable challenge.[19,20] Copper chemistry in oxygenated, aqueous conditions is dominated by the Cu^{2+} cation. Cu^{2+} ions have a d^9 electronic configuration which induces large Jahn-Teller distortion in the first coordination sphere and the additional crystal field stabilisation favours complexes with a 4-coorindate, square planar geometry. The charge density of Cu^{2+}(aq.) ions (ionic radius = 0.80 Å)[21] lies intermediate between hard class A ions and softer class B metal ions. This property means that Cu^{2+} ions favour coordination with chelating ligands that present a mixed donor set with both small, hard donors like N and O, and larger, soft S donors. For this reason, some of the most successful chelates for coordinating Cu^{2+} ions have been developed around *bis*-thiosemicarbazonato-based ligand systems that offer dative covalent bond formation *via* N_2S_2 or N_2SO donor atoms sets (Figure 3).[22] Although tetra-coordinate, square planar complexes with a fully occupied $d(z^2)^2$ orbital stabilise Cu^{2+} ions thermodynamically, ligands like H_2ATSM, and the asymmetric bifunctional version H_2ATSM/A, have two faces of the central metal cation open to solvent.[23] Solvent exposed sites in the first coordination sphere leave complexes like CuATSM susceptible to degradation *via* nucleophilic attack, which can decrease

their overall kinetic/metabolic stability *in vivo*. In the case of copper-based radiotracers, loss of the metal ion from the radiopharmaceutical leads to higher accumulation of radioactivity in background tissues such as the liver, spleen and kidneys. For immuno-PET and immuno-SPECT agents, such instability can complicate analysis and quantification by reducing target specificity and decreasing image contrast. For RIT, off-target accumulation of radioactivity causes a potential problem in terms of dosimetry with the need to avoid radiation dose to background organs to minimise potential side-effects. Therefore, when developing copper-based mAbs, it is of paramount importance to minimise demetallation/transchelation *in vivo*.

Another aspect of copper chemistry that must be taken into account when selecting a suitable ligand is the fact that Cu^{2+} ions undergo facile one-electron reduction to their corresponding Cu^{+} species. While square planar Cu^{2+} complexes are thermodynamically stable due to high crystal field splitting forces, Cu^{+} complexes prefer a tetrahedral geometry and are often far less stable with lower formation constants (log β). Reduced Cu^{+} complexes are also kinetically labile and normally undergo rapid ligand exchange, leading to demetallation and potential loss of the copper ion *in vivo* to competing ligands such human serum albumin, ceruloplasmin and other copper-binding proteins. Single-crystal X-ray structures supported by Density Functional Theory (DFT) calculations have shown that tetra-coordinate Cu^{2+} complexes comprising asymmetric donor atom sets like N_2S_2 *bis*-thiosemicarbazonato ligands induce a twist distortion in the square planar geometry.[23] While structural distortion induces a slight increase in thermodynamic stability of complexes like CuATSM/A, the twisted geometry lies intermediate between true square planar Cu^{2+} complexes and a tetrahedral geometry favoured for reduced Cu^{+} complexes. Hence, geometric distortion facilitates metal-centred reduction of Cu^{2+} complexes to give Cu^{+} species that rapidly demetallate *in vivo* due to their lower thermodynamic, kinetic and metabolic stability. For

this reason, N_2S_2 *bis*-thiosemicarbazonato ligands are typically not employed in the design of long-circulating copper-radiolabelled mAbs. Instead, the majority of copper-radiolabelled mAbs concentrate on stabilising the Cu^{2+} ion, and have been developed around *aza*-macrocyclic-based chelates like NOTA, DOTA and TETA (Figure 3). Other Cu^{2+} chelates incorporate varying combinations of macrocyclic N-donors with other donor groups such as carboxylates, phosphates or heteroaromatic rings such as derivatised pyridines or imidazoles etc.

To best of our knowledge, only two different chelates, BAT and DOTA, have been used in the development of $^{64/67}$Cu-radiolabelled mAbs for imaging and RIT in human trials. In a pioneering Phase I/II clinical trial, Philpott *et al.* investigated the distribution and specificity of a ^{64}Cu-labelled murine mAb, [^{64}Cu]-BAT-2IT-1A3, in 36 patients with suspected advanced primary or metastatic colorectal cancer.[24] Imaging was compared with compared [^{18}F]-FDG and the study found that [^{64}Cu]-BAT-2IT-1A3 was more specific for detecting colorectal tumours than [^{18}F]-FDG which showed false positive indications in patients with inflammatory lesions. The sensitivity of [^{64}Cu]-BAT-2IT-1A3 was found to be 71% per lesion and 86% per patient. The investigation also found that immuno-PET imaging with [^{64}Cu]-BAT-2IT-1A3 offered diagnostic improvements over previously developed radioimmunoscintigraphy imaging using [^{111}In]-HBED-1A3[25] (63% per lesion and 76% per patient). Critically, follow-up studies found no adverse side-effects from ^{64}Cu-mAb administration. However, it was noted that in about 25% of patients, increased titres of human anti-mouse antibody (HAMA) were found. This immune response toward an administered mAb-based radiopharmaceutical can be minimised/avoided by the use of chimeric or fully humanised mAbs. Subsequent pre-clinical studies by Connett *et al*.[26] showed the potential of both ^{64}Cu and ^{67}Cu-radiolabelled BAT-2IT-1A3 for RIT. Small GW39 tumours (~0.2 g) showed 82% and 93% remission in tumour size when treating with 2.0 mCi of ^{64}Cu- or 0.4 mCi

of ^{67}Cu-BAT-2IT-1A3, respectively. Interestingly, larger tumours (~0.6 g) only showed growth inhibition but not regression, even when treating with higher doses of radioactivity. These data highlight an important limitation of using mAb-based drugs that often fail to penetrate fully into the core of larger solid tumours.

In the late 1990s, DeNardo and co-workers reported preclinical[27] studies and clinical translation[13,28,29] of the radiolabelled murine mAb, ^{67}Cu-BAT-2IT-Lym-1, for RIT in patients with Non-Hodgkin's lymphoma (NHL). In one study, O'Donnell *et al*.[28] measured the dosimetry and pharmacokinetics of ^{67}Cu-BAT-2IT-Lym-1 in 12 NHL patients with stage III or IV disease that had failed to respond to standard therapy. Patients received up to 4 separate doses of ^{67}Cu-RIT at 4 week intervals with administered activities between 0.93 – 2.22 GBq/m^2/dose. The trial found that chemotherapy-resistant patients had a combined partial and complete response rate of 58% (7/12 patients). Radiation dosimetry measurements confirmed specificity of radiotracer uptake in tumours which led to disease lesions receiving the highest mean radiation dose (2.35±0.97 Gy/GBq). Measurements also found favourable radiotracer distribution with tumour-to-background organ ratios against marrow lung, kidney and liver of 28:1, 7.4:1, 5.3:1 and 2.6:1, respectively. In a follow-up study, Mirick *et al*.[13] performed detailed analysis of the radiochemical stability of ^{67}Cu-BAT-2IT-Lym-1. Transfer of ^{67}Cu to ceruloplasmin was observed in all patients with an average of 2.8±1.5% of the initial dose being lost to ceruloplasmin in the liver. The release rate of ^{67}Cu from ^{67}Cu-ceruloplasmin in the liver to the blood was 0.9±0.4 %ID/day during the first 3 days post-radiotracer administration. The researchers noted that loss of ^{67}Cu ions to endogenous proteins led to a biphasic clearance rate.

In efforts to increase the metabolic stability of $^{64/67}$Cu-radiolabelled mAbs, Lewis *et al*.[30] compared ^{64}Cu-TETA-1A3 *versus* ^{64}Cu-BAT-2IT-1A3 (Figure 4). Head-to-head experiments

showed that conjugation of the TETA chelate to the mAb *via* amide bond formation led to favourable serum stability, biodistribution, immunoreactivity and dosimetry properties. Alongside earlier work,[31] these data demonstrate the importance of developing new chelating systems to increase the stability of Cu-based radiotracers *in vivo*.

Recent clinical studies using ^{64}Cu-mAbs have tended to employ the DOTA chelate coupled to the mAb *via* amide bond formation. Clinical trials worldwide have reported the efficacy of using ^{64}Cu-DOTA-trastuzumab to measure expression of the human epidermal growth factor 2 (HER2/*neu*) in breast cancer patients.[32–34] In addition, ^{64}Cu-labelled cetuximab for imaging epidermal growth factor receptor (EGFR) has been studied extensive in preclinical work with experiments comparing the performance of different chelates including DOTA,[35,36] CB-TE1A1P, CB-TE1K1P in combination with either tradition amide bond coupling or 'Copper-free Click' methods for rapid bioconjugation.[37] As efforts gather pace to improve access to ^{67}Cu,[18] identification of new chelates, linkers and radiolabelling methods to produce $^{64/67}$Cu-mAbs is essential.

3. **Zirconium radiolabelled antibodies**

Over the last two decades, ^{89}Zr ($t_{1/2}$ = 78.41 h; β+ = 22.74%) has emerged as the most important radionuclide for immuno-PET.[4] Elsewhere in this issue of Journal of Labelled Compounds and Radiopharmaceuticals, Viola-Villegas and co-workers present a detailed overview of progress made in the use of ^{89}Zr-radiolabelled mAbs for clinical imaging. The follow section focuses on the radiochemistry and coordination chemistry of $^{89}Zr^{4+}$ ions. The half-life of just over 3 days matches well with the extended circulation times of mAbs in the human body which facilitates accurate measurements of antibody pharmacokinetics at time points beyond 1 week after radiotracer

administration. The chemistry and radiochemistry of ^{89}Zr offers a number of technological advantages over other radionuclides such as ^{64}Cu. ^{89}Zr is produced *via* low energy (ca. 13 – 15 MeV) proton beam irradiation of commercially available ^{89}Y solid metal foils.[38] The ^{89}Y target material has a natural isotopic abundance of 100%, which unlike ^{64}Cu that requires recycling of isotopically enriched ^{64}Ni electroplated targets, makes production of ^{89}Zr comparatively cheap. Extraction methods are optimised and fully automatable yielding either ^{89}Zr-tetraoxalate ($[^{89}Zr(C_2O_4)_4]^{4-}$) or ^{89}Zr-chloride in high chemical and radiochemical purity, and high specific activity (470–1195 Ci/mmol).

The aqueous phase chemistry of zirconium is limited to the group oxidation state of 4+ with a d^0 electronic configuration. The thermodynamic stability of Zr^{4+} complexes is dominated by electrostatic interactions with no contribution from crystal field stabilisation. The very high charge density of Zr^{4+}(aq.) ions (ionic radius = 0.85 Å)[21] induces significant bond polarisation in the first coordination sphere and the dative bonds have strong 'covalent character'. The very low solubility product of $Zr(OH)_4$ (log K_{sp} = 56.94±0.32)[39] means that Zr^{4+} species have a strong tendency to hydrolyse and form colloidal species *in aquo*. Avoiding precipitation of Zr-oxo species requires the use of metal binding chelates that form exceptionally stable complexes with high-valent metal ions. For this reason, most of the work using ^{89}Zr-mAbs has employed the hexadentate, *tris*-hydroxamic acid chelate, desferrioxamine B (DFO). The formation constant of Zr-DFO has yet to be determined but experience has found that excess Fe^{3+} ions do not transmetallate with the preformed ZrDFO complex on a time scale appropriate for immuno-PET (Holland unpublished data). This observation suggests that either the ZrDFO complex is kinetically stable toward transmetallation with Fe^{3+} ions, and/or that the formation constant of ZrDFO is possibly higher than the reported thermodynamic stability of FeDFO (log β = 30.6).[40]

It is notable that although DFO is an exceptionally powerful chelate for coordination of Zr^{4+} ions, zirconium has the ability to accommodate between 6 and 8 donor atoms in the first coordination. DFT calculations have indicated that DFO fails to fully saturate the first coordination sphere of Zr^{4+} ions and the ligand is quite strained.[41,42] One or two vacant coordination sites are potentially occupied by labile water molecules or anions like chloride. Additional experiments using ^{89}Zr-immuno-PET in rodent models have found elevated levels of activity accumulating in the bone over time. Interestingly, bone activity is typically higher when investigating tumour models that show positive expression of the target antigen than in models where tumour accumulation occurs *via* enhanced permeability and retention (EPR).[41,43–45] These data point toward a specific intratumoural metabolism that leads to recirculation of unidentified Zr^{4+} species that sequester in the bone. Other studies have shown that $[ZrDFO]^+$ is excreted rapidly *via* a renal clearance mechanism yet other species including a putative '^{89}Zr-chloride' in phosphate buffered saline, and $[^{89}Zr(C_2O_4)_4]^{4-}$ accumulate in liver and bone, respectively.[38,46] Collectively, data suggest that ^{89}Zr species with overall anionic charge have a higher propensity to sequester in bone. As previously mentioned for the ^{64}Cu work, further studies are required to elucidate the nature of the radioactive metabolites that recirculate *in vivo* after release from tumours and potentially other background organs like the liver. We note that similar bone sequestration of ^{89}Zr radioactivity has not been reported in human trials. Nevertheless, these preclinical data, combined with the fact that DFO does not fully satisfy the coordination requirements Zr^{4+} ions, have prompted recent efforts in the design and synthesis of alternative chelate systems for this radionuclide.[47] A selection of recent bifunctional chelates that have been developed as potential alternatives to the 'gold standard' DFO chelates are presented in Figure 5.[47–53]

Detailed DFT calculations explored the mechanism of ligand substitution between oxalate and hydroxamate ligands bound to Zr^{4+} ions.[42] This computational study revealed a comprehensive set of 'design criteria' that can aid the synthesis of new chelates for selective, high affinity coordination of Zr^{4+} ions. New ligands should aim to incorporate hard, class A donor atoms in a ligand geometry that is pre-organised for coordination to Zr^{4+} ions. Since Zr^{4+} ions can accommodate between 6- to 8- donor atoms in the first coordination sphere, new chelates should aim to maximise thermodynamic and kinetic stability. Whilst increasing the denticity of a chelate has the general effect of increasing the thermodynamic and kinetic stability of a metal complex due to an increased chelate effect, there is no fixed rule that dictates 7- or 8-coordinate complexes are more stable that 6-coordinate complexes. Rather, the relative thermodynamic stability between 6-, 7- and 8-coorindate complexes is a balance between the generally increased stabilisation acquired through coordination of an extra donor atom *versus* increased repulsive forces generated from increased steric crowding in the first coordination sphere and potentially increased strain induced in the ligand backbone. Furthermore, larger metal ion complexes with 8-coordinate geometries are likely to be more susceptible toward ligand exchange mediated by solvent (water) molecules. For maximum thermodynamic stabilisation of Zr^{4+} ions, ligand scaffolds should be carefully designed to increase the acidity of the donor atoms. This will potentially increase the degree of "covalent-character" bonding between the ligand and $^{89}Zr^{4+}$ ions. To achieve this, donor atoms should be part of strongly acidic groups. Suitable functional groups that have been used in the design of successful Zr^{4+} chelates include carboxylic acids, phosphates, hydroxamic acids, phenols, catechols, and hydroxypyridinonates (Figure 5).

Desferrioxamine B is a natural product produced by bacteria and acts as a siderophore, extracting Fe^{n+} ions from highly insoluble iron oxides (the log K_{sp} ($Fe(OH)_3$ lies between 10^{-37} and

10^{-44} depending on the conditions).[54] Extracting iron from soil requires very powerful chelates which can pose a potential problem for radiochemistry with $^{89}Zr^{4+}$ ions. While $[Zr(DFO)]^{+}$ is stable with respect to transmetallation by Fe^{3+} ions, care must be taken to ensure that no iron contaminants are present in any of the solutions used for $^{89}Zr^{4+}$ extraction or radiolabelling. Experience has found that trace amounts of Fe^{3+} ions act as efficient 'poisons' toward ^{89}Zr radiochemistry. Since the majority of new chelates designed for coordination of $^{89}Zr^{4+}$ ions are based on, or inspired by, the structures of siderophores, working with high-purity metal ion free solutions is essential to ensure that radiolabelling proceeds efficiently, and generates products with high radiochemical purity and effective specific activity. In spite of these challenges, efficient protocols have been reported for producing many ^{89}Zr-DFO-mAbs.[43,55] We note that although several bifunctional chelates have been produced and claimed to be superior in terms of radiochemical stability toward transchelation of Zr^{4+} ions, it is yet to be seen if any of these new ligands will emerge as a genuine competitor to DFO. In the clinical setting, DFO has a number of strong advantages that present a very high barrier for any alternative chelate to cross. For instance, DFO is a US-FDA approved drug, it is readily available and cheap, has good solubility properties (unlike many new chelates), and chemical methods for attaching DFO to mAbs are highly reproducibly, efficient and now practiced as routine in many radiochemistry facilities. As clinical trials using ^{89}Zr-DFO-mAbs accelerate, and generally image quality from reported clinical trials is considered excellent with no loss of radiometal to the bone, these positive experiences will make many physicians reluctant to venture into uncharted waters without obvious need or benefit. In addition, the costs of generating essential toxicological studies of a new chelate prior to clinical translation may prove prohibitive for most second-generation chelates. The question that must be

addressed by any new radiotracer (or here chelate) is, how much better must a new tool be to cause the Nuclear Medicine community to shift from a well-established, reliable and trusted technology?

While the ability to image mAb distribution over the course of several weeks can be considered an advantage, the major limitations of ^{89}Zr-mAbs are the comparatively poor dosimetry profile and the practical challenges of managing patients who receive a ^{89}Zr radiotracer injection and remain radioactive for extended periods of time. Long circulation times with limited excretion mean that ^{89}Zr-mAb radiotracer doses are limited to ~185 MBq[56–58] with typical doses of, for example, ^{89}Zr-DFO-trastuzumab for imaging HER2/*neu* expression in breast cancer patients around 37 MBq/patient. As an initial tool to validate the usefulness of a new biomarker, ^{89}Zr-mAbs remain an excellent choice. However, as alternative radiotracers based on small-molecules are developed to image the same targets, for example ^{68}Ga-urea-based Glu-NH-C(O)-NH-Lys compounds for PET imaging of prostate-specific membrane antigen (PSMA) agents, practical considerations are likely to dictate the long-term future of ^{89}Zr-mAbs.

4. **Gallium-67 radiolabelled antibodies**

Gallium-67 radiolabelled mAbs were amongst some of the first antibody-based radiotracer tools developed for radioimmunoscintigraphy and immuno-SPECT.[59] The radiochemical properties of ^{67}Ga ($t_{1/2}$ = 3.26 d; ε = 100%), with intense Auger electron emissions and various γ-rays emitted in the range 8 – 887 keV make this radionuclide suitable for both imaging and RIT with mAbs. Similar to ^{89}Zr, $^{67}Ga^{3+}$ exist in the group oxidation state with no redox chemistry. The thermodynamic stability of Ga^{3+} complexes is dominated by electrostatic interactions with a strong preference for hexadentate chelates proffering hard, class A donor atoms. In addition, the high charge density of Ga^{3+} ions (ionic radius = 0.62 Å)[21] leads to a high propensity of Ga complexes

to hydrolyse in aqueous solution, potentially forming Ga-colloidal species of uncertain chemical composition. Stabilising Ga^{3+} ions against rapid hydrolysis and formation of either gallium tetrahydroxide anions ($Ga(OH)_4^-$) or Ga-colloids requires careful control of the reaction buffer composition, ionic strength and pH, and the use of chelates that form Ga complexes with very high formation constants. Chelates of choice for Ga^{3+} radionuclides include bifunctional derivatives of DFO, EDTA and various *aza*-macrocycles primarily based on the structures of NOTA and DOTA (Figures 3 and 5). Indeed, Koizuma *et al*. reported efficient radiolabelling of ^{67}Ga-DFO-mAbs in 1988. Interestingly, they also tested the stability of different coupling strategies and found that the use of glutaraldehyde coupling led to high non-specific uptake in liver and spleen. In contrast, ^{67}Ga-DFO-mAbs linked *via* thioether bonds (maleimido chemistry) displayed the highest tumour-to-liver ratios, and radiotracers produced using disulphide bridges were unstable, with activity cleared rapidly from circulation. Nowadays, alternative methods for mAb coupling and different chelates for Ga^{3+} ion coordination are available but DFO remains a competitive choice.[60] With a prevailing shift toward immuno-PET, development of ^{67}Ga-mAbs has stagnated in recent years. Nevertheless, as research efforts aimed at delivering an Auger-emitting radionuclide to the cell nucleus intensify, ^{67}Ga has potential to see a resurgence in interest. A recent article by Othman *et al*. reassessed the therapeutic potential of ^{67}Ga and concluded that on a per cell basis, ^{67}Ga causes as much damage as ^{111}In to plasmid DNA.[61]

5. **Indium-111 radiolabelled antibodies**

Since the 1980s, ^{111}In-radiolabelled mAbs have been developed as tools for radioimmunoscintigraphy, immuno-SPECT and for RIT. The radionuclide ^{111}In ($t_{1/2}$ = 2.80 d; ε = 100%) decays with intense low energy Auger electron emission (2.72 keV, 100%) and also emits

a number of γ-rays whose energy and intensity (171 keV [90.7%]; 245 keV [94.1%]) are ideally suited for high resolution SPECT imaging and targeted RIT.

In the following examples of ^{111}In-mAbs, DTPA was used as the chelate for coordination of the $^{111}In^{3+}$ ion. Indium lies underneath gallium in group 13 (group 3A) of the Periodic Table. As such, the chemistry of In^{3+} and Ga^{3+} ions are quite similar. One notable difference is that In^{3+} ions have a larger ionic radius (0.80 Å)[21] and can accommodate additional donor atoms in the first coordination sphere. In this regard, the coordination requirements of $^{111}In^{3+}$ lie between Ga^{3+} and Zr^{4+} ions, and for this reason, DTPA (which offers up to nine, class A, hard donor atoms) remains the primary chelate used for $^{111}In^{3+}$ coordination. To the best of our knowledge, little work has been reported on the development of alternative chelates for specific coordination of $^{111}In^{3+}$ ions. However, as discussed for ^{67}Ga, the resurgence of interest in targeted RIT using Auger emitters is likely to stimulate radiochemists to revisit the coordination chemistry and radiochemistry of ^{111}In.

Indeed, early clinical studies reported by Ryan *et al*.[62] found that imaging was able to detect breast lesions in breast cancer patients infused with varying doses of different human IgM monoclonal antibodies ^{111}In-YBB-190, ^{111}In-YBB-209 or ^{111}In-YBB-088. However, antigen expression levels and mAb dose were critical factors in determining the success of diagnostic imaging with ^{111}In-mAbs.

One of the earliest radiolabelled mAbs to receive US-FDA approval (in 1996) for imaging was ^{111}In-capromab pendetide (^{111}In-7E11; ProstaScint®). ^{111}In-capromab pendetide is a mouse mAb that recognizes a specific intracellular epitope of prostate specific membrane antigen (PSMA) and can be used for immuno-SPECT imaging of prostate cancer soft tissue metastases. Unfortunately, targeting an intracellular epitope led to sub-optimal performance of this radiotracer in clinical diagnosis of prostate cancer with fairly low sensitivity for viable tumour lesions (62%

for lymph node metastases; 50% for prostate bed recurrence). Furthermore, ^{111}In-capromab pendetide was not able to identify prostate cancer lesions in bone which is the most common site of metastatic disease in this patient population. Subsequent preclinical and clinical studies using ^{89}Zr-DFO-J591 to image an extracellular epitope of PSMA mean that ^{89}Zr-immuno-PET has largely superseded the need for ^{111}In-ProstScint scans. Despite limitations, ^{111}In-capromab pendetide remains available on the market.

Several other ^{111}In-mAbs have previously received US-FDA approval include ^{111}In-satumomab pendetide (OncoScint®) for imaging TAG-72, a tumour-associated antigen found on ~95% of colorectal carcinomas and 100% of ovarian carcinomas; ^{111}In-imiciromab-pentetate (MyoScint®), a murine mAb Fab-fragment directed against human cardiac myosin and formerly used for cardiac imaging; ^{111}In-igovomab (Indimacis-125®), a mouse F(ab')$_2$ fragment for imaging carcinoma antigen 125 (CA-125) in the diagnosis of ovarian cancer. However, each of these ^{111}In-radiotracers has subsequently been withdrawn.[2]

6. **Technetium-99m radiolabelled antibodies**

Technetium-99m ($t_{1/2}$ = 6.01 h; IT = 100%) is the most common radionuclide used to develop SPECT radiotracers.[63] In contrast to many other radionuclides described here, the chemistry of ^{99m}Tc is highly diverse. Technetium lies in group 7B of the Periodic Table, underneath manganese, and as such, exhibits a rich redox chemistry. ^{99m}Tc species in a wide range of oxidation states from –1 to +7 have been reported. Variable oxidation states mean that Tc complexes are potentially redox active, implying that ^{99m}Tc-complexes must be designed to be thermodynamically and/or kinetically stabile toward redox reactions *in vivo*. The majority of radiotracers have been

developed around $^{99m}Tc^{5+}$ and $^{99m}Tc^{+}$ ions. A unique feature of ^{99m}Tc radiochemistry is the concept of utilising different '^{99m}Tc-cores' with the three most common being {^{99m}Tc=O}, {$^{99m}TcO_3$} and {$^{99m}Tc(CO)_3$} (Figure 6).[63]

During the mid-1990s to mid-2000s, a number of ^{99m}Tc-mAbs received market approval.[2] For example, ^{99m}Tc-nofetumomab merpentan (Verluma®) is a mouse mAb Fab-fragment attached to a merpentan chelate and used for imaging the pan-carcinoma glycoprotein antigen EpCAM and/or CD20/MS4A1 in cancers of the lung, gastrointestinal tract, breast, ovary, pancreas, cervix, kidney and bladder. Verluma® was approved in 1996 but withdrawn in 1999. ^{99m}Tc-arcitumomab (CEA-Scan®) is a mouse Fab' fragment developed by Immunomedics to target the Carcinoembryonic antigen (CEA) cell-adhesion proteins which are biomarkers on various cancers including colorectal tumours. CEA-Scan® was approved in 1996 but withdrawn in 2005. ^{99m}Tc-sulesomab (LeukoScan®) received approval in 1997 and is a mouse Fab' fragment that targets granulocyte cell antigen NCA-90 and is used for imaging infections and inflammations in patients with suspected osteomyelitis. LeukoScan® is also being investigated in the evaluation of soft tissue infections.[64] ^{99m}Tc-votumumab (HumaSPECT®) is a human monoclonal antibody for detection of 3-fucosyl-*N*-acetyl-lactosamine (CD15) expression in colorectal tumours. Although HumaSPECT® received approval in 1998, it was withdrawn in 2004 without being made available on the market. Finally, ^{99m}Tc-fanolesomab (NeutroSpec®) is a mouse mAb developed to target CD15 and received approval in 2004 for diagnosis of appendicitis. However, in December 2005 the US-FDA issued an alert and NeutroSpec® marketing was voluntarily suspended due to reports of serious and life-threatening cardiopulmonary events that followed immediately after NeutroSpec® administration. Two deaths were reported and further patients experiences serious complications including cardiac arrest, hypoxia, dyspnea and hypertension. While these adverse

reactions were most likely due to a reaction to the antibody-component and not the radionuclide, it offers a lesson that, as with chemotherapeutic drugs, full preclinical characterisation of radiotracers is crucial before translation to the clinic.

7. **Iodine radiolabelled antibodies**

Although not radiometals, iodine radionuclides remain among the most frequently utilised therapeutic isotopes in the clinic. The radionuclide of primary interest is ^{131}I due to its dual emission capabilities. ^{131}I ($t_{1/2}$ = 8.1 d) emits β– particles (average energy of 192 keV with a range of 0.8 mm in tissue) as well as a concomitant γ-emission (364 keV) suitable for SPECT imaging.[65] ^{131}I is a reactor-produced isotope, conveniently accessible from ^{235}U fission products.[66] However, ^{123}I and ^{125}I have also become of interest due to their potential for either imaging or Auger therapy applications, respectively. The photon energy of ^{125}I is considered too low for optimal imaging, especially for quantitative imaging, and its half-life is undesirably long. Thus, ^{125}I is typically used for *in vitro* applications and radioactive binding assays.[67] ^{124}I ($t_{1/2}$ = 4.2 days) has a relatively low ratio of disintegration resulting in positrons (about 23%), and a complex decay scheme which includes high-energy gamma emissions (highest about 1.7 MeV). It is typically produced by using enriched ^{124}Te *via* the ^{124}Te(d,2n)^{124}I reaction or in recent years, the ^{124}Te(p,n)^{124}I reaction.[68]

In contrast to radiolabelling with metal ions, incorporation of iodine radionuclides requires formation of covalent bonds. Typically, radioiodine is introduced using mild oxidative reagents that minimise potential chemical degradation of mAbs. Chloramine-T (*N*-chloro-*p*-toluene sulfonamide) is an aromatic oxidising agent commonly used for this purpose, but requires close monitoring and quenching of the reaction before excessive mAb oxidation occurs (Figure 7).[69] The use of solid-support chloramine-T provides a milder radiolabelling alternative, allowing for

filtration workups as a way to rapidly remove the oxidant.[70] Another commonly used oxidizing agent employed is iodogen (1,3,4,6-tetrachloro-3α,6α-diphenylglycoluril).[71] Other methods involve radioiodination of an activated-ester small molecule (*N*-succinimidyl 3-(4-hydroxyphenyl) propionate; Bolton-Hunter reagent) with chloramine-T, followed by mAb conjugation in a secondary step.[72]

[^{131}I]NaI-mediated treatment of malignant thyroid disorders has represented a mainstay of RIT in the clinic. Recently, ^{131}I-mAbs are becoming of greater interest for targeted cancer therapy. ^{131}I-tositumomab (Bexxar®) is the earliest representative of this compound class. ^{131}I-tositumomab is used to treat certain types of NHL.[73] Investigations have also sought define the role of ^{131}I-tositumomab RIT in treating Hodgkin's lymphoma, diffuse large B-cell lymphoma,[74] and multiple myeloma.[75] Based on the promising outcomes in clinical studies, ^{131}I-tositumomab was approved by the FDA for clinical practice in patients with lymphoma. ^{131}I-Lym-1 (Oncolym®) is an ^{131}I-radiolabelled mAb in Phase III clinical trials for non-Hodgkin's lymphoma.[76] Cotara® is a genetically engineered chimeric human/mouse mAb that binds to the DNA-histone H1 complex, targeting the necrotic core of solid tumours.[77] Phase II clinical trials on patients with astrocytoma, brain gliobastoma, hepatocellular carcinoma (HCC) have shown promising results.[78] Similarly, the treatment was also found to be successful in lung cancer patients *via* intratumoral injections.[79]

Until recently, iodine-124 was not considered to be an attractive isotope for medical applications owing to its complex radioactive decay scheme, which includes several high-energy γ-rays. Limited availability of this radionuclide has also impeded its clinical application. Among clinically assessed ^{124}I-radiotracers, sodium [^{124}I]-iodide is potentially useful for diagnosis and dosimetry in thyroid disease and [^{124}I]-M-iodobenzylguanidine ([^{124}I]-MIBG) has shown promise for cardiovascular imaging as well as dosimetry of malignant diseases such as neuroblastoma,

paraganglioma, pheochromocytoma, and carcinoids.[80] A number of monoclonal antibodies have been labelled with ^{124}I and imaged successfully in mouse models.[81,82] As with several other radionuclides, interest in ^{124}I-mAbs has waned in light of the success of ^{89}Zr-mAbs in preclinical and clinical settings.

8. **Yttrium radiolabelled antibodies**

^{90}Y is a widely used radiometal for β^- therapy. With a half-life of 2.67 days, it decays *via* β^- emission (100%) with a maximum β-particle energy of 2.288 MeV, providing a greater penetration range *in vivo* than many other β^- emitting nuclides.[12,83] ^{90}Y may be produced using various nuclear reactions. Irradiation of ^{89}Y in a nuclear reactor produces ^{90}Y, however, this route generates an ^{90}Y product with low specific activity that is inseparable from the target material. No-carrier added ^{90}Y can be obtained by separation of ^{90}Y from ^{90}Sr ($t_{1/2}$ = 28.5 y). Currently, the separation of ^{90}Y is carried out at production sites, and the long half-life of ^{90}Sr could enables manufacture of a generator system comparable to the ^{99}Mo generator for ^{99m}Tc. ^{90}Sr is one of the most abundant fission product radionuclides in spent nuclear fuel as it is generated in high yield.[84] The high β^- energy renders ^{90}Y suitable for treatment of larger, poorly vascularized tumours (approximate β^- range of ~12 mm in addition to extended therapeutic range through the "crossfire effect"). More recently, in addition to accessibility of ^{90}Y as a therapeutic isotope, the PET isotope ^{86}Y has emerged as the imaging congener. Currently, primary limitations of use of ^{86}Y clinically are its non-ideal emission characteristics: β^+ emissions (2.019, 2.335 MeV) are sub-optimal for imaging due to their high energy leading to decreased image resolution, and poor radiation dosimetry profile arising from high-energy γ–ray emissions (1.077, 1.153, 1.854, 1.921 MeV).[85]

Y^{3+} has an ionic radius of 1.02 Å, an absolute electronegativity of 41.2 eV and a hardness of 20.6 eV.[86] It ranks among the hardest trivalent ions, exhibiting a strong preference for oxygen and nitrogen donors. Most frequently used chelates for coordination of $^{86}Y/^{90}Y$ are DOTA[87] and CHX-A″-DTPA[88] (Figure 3). Main issues identified with these established ligand systems include slow complexation kinetics at room temperature (DOTA), and/or decreased stability *in vivo* (DTPA-derivatives).[89] To leverage the enhanced kinetic stability of macrocycles and rapid chelation of acyclic systems, Kang *et al*. have synthesised the bimodal ligands 3p-C-NETA and 3p-C-DEPA (Figure 8) that possess both macrocyclic and acyclic moieties for cooperative metal ion binding. Radiolabelling of these chelates also shows favourable radiochemical yields under mild conditions (room temperature, pH 5.5, 60 min).[90] However, only 3p-C-NETA exhibited sufficiently high kinetic stability in plasma challenge experiments. Price *et al.* evaluated the acyclic bifunctional chelator p-NCS-Bn-octapa-NCS (Figure 8) in comparison with CHX-A″-DTPA and found that the ^{90}Y-octapa complex exhibited increased plasma stability while maintaining equivalent *in vivo* performance when conjugated to trastuzumab.[91]

The 64-hour half-life and therapy-avid, γ-emission-free nuclear properties have contributed to the clinical success of ^{90}Y in recent years. Ibritumomab tiuxetan (Zevalin®) is an FDA-approved ^{90}Y-radiolabelled mAb that combines DTPA linked to ibritumomab, allowing for the targeted irradiation with β-particles in B cell non-Hodgkin's lymphoma.[92] A number of new ^{90}Y-labelled mAbs and antibody fragments are currently being assessed for efficacy in clinical trials. ^{90}Y-labelled basiliximab and daclizumab[93] for Non-Hodgkin lymphoma, as well as ^{90}Y-labelled microbeads (under the trade names TheraSphere and SIR-Spheres) have obtained FDA approval in 1999 and 2002 for the treatment of non-resectable liver cancer and other applications of radioembolization.[94] CD22-targeting ^{90}Y-labelled epratuzumab is currently evaluated in a Phase

III trial for the treatment of lymphoma, leukaemia and some immune diseases.[95] Work by Salako and co-workers investigating ^{90}Y-BAT-Lym1 in comparison with the ^{131}I and ^{67}Cu-labeled analogue showed decreased efficacy when compared with Lym1 labelled with other therapeutic isotopes.[96] Beyond mAb-based agents, ^{90}Y-labelled DOTATOC (somatostatin-conjugate) is also under clinical investigation for the treatment of larger neuroendocrine tumours.[97]

9. **Lutetium-177 radiolabelled antibodies**

^{177}Lu ($t_{1/2}$ = 6.6 days) is a mixed mode β^- and γ–ray emitting radionuclide. It decays with emission of β^- particles of 176 (12%), 384 (9%), and 497 keV (79%) as well as γ–rays with energies of 208 (11%) and 113 (6.6%) keV rendering this isotope suitable for SPECT imaging and RIT.[83] ^{177}Lu is typically obtained using reactors by neutron irradiation of ^{176}Lu to afford ^{177}Lu in high yields,[98] satisfactory specific activities. However, reactor production yields both the desired ^{177g}Lu and the excited state ^{177m}Lu as a radionuclidic impurity. ^{177}Lu can also be produced by neutron activation of enriched ^{176}Yb to afford ^{177}Yb (1.9 h half-life), which then decays to ^{177}Lu.[99] This synthesis produces higher specific activities and a no-carrier added product, which more desirable for the labelling and *in vivo* imaging of low-abundance biological targets. The β^- emission of ^{177}Lu has an approximate range of 2 mm *in vivo*, ideal for irradiation of smaller tumours and metastases.

As the element with the greatest number of protons of the lanthanide series, Lu^{3+} experiences the strongest Lanthanide contraction of ionic radius, ranging from 0.98 Å (coordination number 8) or 1.03 Å (coordination number 9). Lu^{3+} can be considered a hard Lewis acid with an absolute electronegativity of 33.1 eV and a hardness of 12 eV.[86] Depending on the steric crowding of the coordinating chelate, Lu^{3+} ions commonly form complexes of coordination number 8 or 9. Both cyclic and acyclic chelators have been utilised for this metal ion, specifically

DTPA, CHX-DTPA and DOTA.[100,101] The slow rate of complexation of DOTA-based ligands with ^{177}Lu becomes a significant disadvantage for preparation of DOTA-based radiopharmaceuticals. For this reason, heating becomes essential in most cases in order to increase the complexation rate Generally, heating at 95 °C for 25–30 min is performed in order to achieve near quantitative radiolabelling yields for the preparation of ^{177}Lu–DOTA-conjugated somatostatin analogues. DOTA–affibodies have been radiolabelled with ^{177}Lu under heating at lower temperature (60 °C) to obtain high-efficiency labelling. Whole antibodies are typically labelled either at room temperature or 37 °C, in order to not jeopardise the integrity of the protein. Typically, this results in less than quantitative radiochemical labelling yields for ^{177}Lu-mAbs or the need to employ reaction times of 1 hour or longer to achieve quantitative complexation of the radionuclide. Once DOTA-type complexes are formed, they exhibit high kinetic and thermodynamic stability, with no significant dechelation reported *in vivo*, even after long circulation times typical for mAbs. The chelates 3p-C-NETA and 3p-C-DEPA (Figure 8) as synthesized by Kang *et al*.[90] and evaluated with ^{90}Y (*vide supra*) have also shown promise, with near-quantitative ^{177}Lu labelling yields under mild conditions (room temperature, pH5.5, 60 min). The trastuzumab conjugate of 3p-C-NETA showed high *in vivo* stability, high tumour uptake and low accumulation in off-target organs. Similarly, trastuzumab conjugates with the acyclic octadentate chelator p-SCN-Bn-octapa (Figure 8) can be labelled with ^{177}Lu at room temperature within 15 minutes.[102] This is in contrast with the corresponding DOTA conjugate, which requires 37 °C and extended reaction times (60 min.) to achieve 85% radiochemical yield. Both of these trastuzumab conjugates exhibited identical behaviour *in vivo*. Octapa-derivatives represent a ligand class that provides an attractive alternative to ‘gold standard’ DOTA derivatives due to their improved radiolabelling characteristics.

The extent of preclinical studies has been reviewed by Banerjee *et al*.[103] In terms of clinical studies, ^{177}Lu has witnessed increasing use. The 6.6 day half-life is suitable for use with both peptides and mAbs as targeting vectors. The long half-life is also suitable for access to ^{177}Lu-therapy in hospitals that do not have access to reactor or cyclotron facilities. The non-quantitative radiolabelling yields of ^{177}Lu with mAb conjugates due to sub-optimal radiolabelling protocols to is one potential reason that has limited a more wide-spread adoption of ^{177}Lu-mAbs in the clinic. Beyond mAb-based agents, ^{177}Lu-DOTATOC/DOTATE has been found to be highly effective for the treatment of neuroendocrine tumours and is currently under regulatory review,[104,105] while the imaging-only analogue ^{68}Ga-DOTATE (NETSPOT®) obtained FDA approval in 2016.

10. **Lead-212 radiolabelled antibodies**

^{212}Pb is produced by the decay chain originating from ^{232}U (^{228}Th decay chain) and can be obtained from a generator made from ^{224}Ac or ^{224}Ra. ^{212}Pb ($t_{1/2}$ = 10.6 h) is a β-emitter (100%, 570 keV), but is primarily of interest as the parent nuclide of the α-emitting short-lived ^{212}Bi ($t_{1/2}$ = 60.6 min) and ^{212}Po ($t_{1/2}$ = 0.3 μs) with deposited energies of 21.1% from the 6.2 MeV ^{212}Bi α-particle emission and 67.3% from the 8.9 MeV ^{212}Po α-particle emission.[106] ^{212}Pb/^{212}Bi is considered an *in vivo* generator system.[107] ^{212}Pb itself can be obtained by way of the ^{224}Ra/^{212}Pb generator. However, the short half-life of ^{224}Ra ($t_{1/2}$ = 3.7 d) requires frequent replacement in a clinical setting, similar to the ^{99}Mo/^{99m}Tc generator system.[108] The original generator system was developed in 1989, but in recent years, rekindled interest in α-therapy has resulted in commercial availability.

Pb^{2+} is a post-transition group 14 metal with ionic radius of 1.29 Å, an electronegativity of 23.5 eV and an absolute hardness of 8.5 eV while Bi^{3+} is a group 15 metal with an ionic radius of 117 ppm and an absolute hardness of 10.0 eV.[86] The chelation chemistry of ^{212}Pb faces the

challenge of having to conform to the coordinative preferences of not just Pb^{2+} but also Bi^{3+}. An additional challenge is posed by the emission of Auger electrons and high recoil energy upon decay to ^{213}Bi which can result in significant radiochemical degradation to the conjugated biomolecule. Initial studies using DOTA conjugates indicated loss of ^{212}Pb from the bioconjugate and thus enhanced radiotoxicity.[109] TCMC (Figure 8), a tetramide analogue of DOTA was developed and found to exhibit enhanced kinetic stability with both Pb^{2+} and Bi^{3+}. The bifunctional, backbone-functionalised version of TCMC has been successfully utilised for conjugation to mAbs and subsequent preclinical and clinical application.[110]

Prominent early preclinical studies with $^{212}Pb/^{212}Bi$ include treatment of EL-4 ascites and more contemporarily successful peptide-based metastatic melanoma treatment.[111] A study on treatment of breast cancer xenografts with trastuzumab-linked ^{212}Pb-TCMC showed highly promising outcome, providing the basis for human trials.[112] A Phase I trial of ^{212}Pb-TCMC-trastuzumab for treatment of HER2-overexpressing cancers has recently been completed.

11. **Bismuth-213 radiolabelled antibodies**

^{213}Bi is a short-lived isotope ($t_{1/2}$ = 45.6 min) and decays by α emission (2%, 5.8 MeV) followed by two β emissions, or β emission (98%) followed by an α emission (8.4 MeV) and subsequent β emission to stable ^{209}Bi. In addition, a 440 keV (26%) photon can be utilised for dosimetry *via* imaging. ^{213}Bi can be obtained from ^{225}Ac as part of the $^{225}Ac/^{213}Bi$ generator.[113] A clinically-used generator has been developed and is commercially available for the supply of ^{213}Bi.

The properties of the Bi^{3+} ion have been described in the ^{212}Pb section (*vide supra*). In the case of ^{213}Bi, no prior coordination of a softer metal ion is required as ^{213}Bi is directly eluted from the $^{225}Ac/^{213}Bi$ generator. Thus, bifunctional versions of DOTA are suitable for the incorporation

of ^{213}Bi into targeting vectors, but are often found to exhibit slow chelation kinetics at room temperature, and therefore, are not compatible with mAbs.[114] DTPA chelates ^{213}Bi more rapidly but the resultant 213Bi-DTPA complex exhibits low kinetic stability.[115] Recent efforts have produced mixed macrocyclic systems with acyclic donor components (3p-C-NETA, 3p-C-DEPA, Figure 8) that provide more rapid chelation and enhanced kinetic stability of the resulting radiochemical complex.[90,114] Ideal radiolabelling conditions encompass pH5.5 at room temperature. Another chelating system developed specifically for the Pb^{2+}/Bi^{3+} pair is Me-do2pa by Lima *et al*. which displays favourable complexation kinetics and high thermodynamic stability. Additional radiochemical studies are underway.[116,117]

The short half-life of ^{213}Bi is not ideally matched with the typical pharmacokinetics of mAbs. However, a preclinical study with ^{213}Bi-labelled J591 (antibody against PSMA) found complete inhibition of tumour growth, outlining the potential of this conjugate for application in humans.[118] ^{213}Bi-lintuzumab (^{213}Bi-HuM195 for acute myeloid leukaemia) was part of a clinical trial, and used in combination therapy with chemotherapy.[119] Recent applications of ^{213}Bi are centred on more rapidly targeting vectors such as DOTATOC/DOTATE and PSMA-617.[120,121]

12. **Actinium-225 radiolabelled antibodies**

^{225}Ac has a 10-day half-life and decays to its short-lived daughter isotope ^{213}Bi, also an α-emitter. ^{225}Ac is provided by three main suppliers: the Institute for Transuranium Elements in Germany, Oak Ridge National Laboratory in USA and the Institute of Physics and Power Engineering in Obninsk, Russia. The current worldwide production of ^{225}Ac is approximately 1.7 Ci per year, which would only provide treatment for a small 100-200 patient cohort. Thus, new or more efficient methods of ^{225}Ac production and isolation are needed. The common approach for ^{225}Ac

production is separation from its mother nuclide ^{229}Th (a daughter of ^{233}U) or irradiation of ^{226}Ra or a thorium target with protons in a cyclotron.[122] ^{225}Ac decays[123] to a cascade of 6 daughters until stable ^{209}Bi is obtained, producing in total 4 α- and 3 β- emissions. Some of the intermediate daughters in the decay include ^{221}Fr ($t_{1/2}$ =4.8 min), ^{217}At ($t_{1/2}$ = 32.3 ms), and ^{213}Bi ($t_{1/2}$ = 45.6 min), each of which emits an α-particle. ^{213}Bi also emits a 440 keV γ-ray suitable for imaging.

The lack of stable isotopes of actinium has provided few opportunities to study its coordinative properties. However, recent EXAFS studies have shed light on some characteristics of Ac^{3+} as well as coordinative preference. Ac^{3+} has an ionic radius of 1.12 Å, and absolute hardness of 14.5 eV.[86] XAFS studies on the Ac^{3+} (aq.) complex revealed a coordination number of 10-11, predicting a need for polydentate chelators beyond the usual octadentate DTPA and DOTA-type chelators.[124,125] Limited studies have been carried out on the development of novel chelators for this radionuclide, but reported work includes extended polyaza-macrocycle systems HEHA and PEPA.[126] However, radiolabelling properties and *in vivo* stability did not significantly improve when compared with DOTA, underscoring the need for novel, custom bifunctional chelators for Ac^{3+}. This need has been addressed by recent work from Wilson and co-workers by development of the extended macrocyclic chelator macropa (Figure 8) and its bifunctional analogue. Macropa incorporates ether and amino donors within the macrocycle as well as bidentate picolinate donor arms to match the size and hardness of Ac^{3+}, showing promise for targeted applications.[127]

Due to the limited access to ^{225}Ac, only a handful of human studies have been carried out, but both preclinical and clinical work on therapeutic applications of this isotope has provided promising treatment outcomes. Multiple clinical trials involving ^{225}Ac lintuzumab, an anti-CD33 mAb (HuM195) for the treatment of acute myeloid leukemia are on-going, taking advantage of the

multi-daughter decay scheme of ^{225}Ac as an advantage over the ^{213}Bi-analogue; Preliminary data shows a three orders of magnitude greater potency of ^{225}Ac-HuM195 when compared with ^{213}Bi-HuM195 (www.clinicaltrials.gov).[128]

13. **Conclusion**

The wide range of nuclear properties and half-lives of radiometals represent a tremendous opportunity to develop the next generation of imaging agents and therapeutics for personalised medicine. As the number of radiopharmaceuticals for imaging in the clinic increases, the switch in focus from diagnostic imaging to targeted radiotherapy is likely to continue in the near future. Given the importance of mAbs as biologics, radiotracers for RIT are set to become more prominent players in the nuclear medicine arsenal. In this context, as the personalised medicine gains traction, the need for radiometals will grow. The combination of imaging (pharmacokinetics, clearance, dosimetry) to optimize subsequent therapy provides a unique approach to treatment planning and will lead to an increased number of favourable clinical outcomes. Currently, there is need for new bifunctional chelates that offer improved radiolabelling characteristics for many radiometal systems including established radionuclides like ^{64}Cu, ^{67}Ga, ^{89}Zr, ^{111}In and ^{177}Lu, as well as emerging radionuclides like ^{212}Pb and ^{225}Ac. Progress in this arena is key to propel non-standard radionuclides into the mainstay of nuclear medicine, radiology and oncology.

14. **Acknowledgements**

JPH thanks the Swiss National Science Foundation (SNSF Professorship PP00P2_163683), the European Research Council (ERC-StG-2015, NanoSCAN – 676904) and the University of Zurich for financial support. EB thanks Stony Brook University for start-up funding, as well as NHLBI for a K99 Pathway to Independence award (K99HL125728).

References

(1) Wu, A. M.; Senter, P. D. *Nat. Biotechnol.* **2005**, *23* (9), 1137.

(2) Walsh, G. *Nat. Biotechnol.* **2010**, *28* (9), 917.

(3) Boswell, C. A.; Brechbiel, M. W. *Nucl. Med. Biol.* **2007**, *34* (7), 757.

(4) Moek, K. L.; Giesen, D.; Kok, I. C.; de Groot, D. J. A.; Jalving, M.; Fehrmann, R. S. N.; Lub-de Hooge, M. N.; Brouwers, A. H.; de Vries, E. G. E. *J. Nucl. Med.* **2017**, *58* (Supplement 2), 83S.

(5) Warram, J. M.; De Boer, E.; Sorace, A. G.; Chung, T. K.; Kim, H.; Pleijhuis, R. G.; Van Dam, G. M.; Rosenthal, E. L. *Cancer Metastasis Rev.* **2014**, *33* (2–3), 809.

(6) Milenic, D. E.; Brady, E. D.; Brechbiel, M. W. *Nat. Rev. Drug Discov.* **2004**, *3* (6), 488.

(7) Dennler, P.; Fischer, E.; Schibli, R. *Antibodies* **2015**, *4* (3), 197.

(8) Agarwal, P.; Bertozzi, C. R. *Bioconjug. Chem.* **2015**, *26* (2), 176.

(9) Zeglis, B. M.; Davis, C. B.; Aggeler, R.; Kang, H. C.; Chen, A.; Agnew, B. J.; Lewis, J. S. *Bioconjug. Chem.* **2013**, *24* (6), 1057.

(10) Price, E. W.; Orvig, C. *Chem. Soc. Rev.* **2014**, *43* (1), 260.

(11) Fleuren, E. D. G.; Versleijen-Jonkers, Y. M. H.; Heskamp, S.; van Herpen, C. M. L.; Oyen, W. J. G.; van der Graaf, W. T. A.; Boerman, O. C. *Mol. Oncol.* **2014**, *8* (4), 799.

(12) Holland, J. P.; Williamson, M. J.; Lewis, J. S. *Molecular Imaging*. 2010, pp 1–20.

(13) Mirick, G. R.; O'Donnell, R. T.; Denardo, S. J.; Shen, S.; Meares, C. F.; Denardo, G. L. *Nucl. Med. Biol.* **1999**, *26* (7), 841.

(14) Mcdevitt, M. R.; Finn, R. D.; Sgouros, G.; Ma, D.; Scheinberg, D. A. *Appl. Radiat. Isot.* **1999**, *50*, 895.

(15) Ruggiero, A.; Villa, C. H.; Holland, J. P.; Sprinkle, S. R.; May, C.; Lewis, J. S.;

Scheinberg, D. A.; McDevitt, M. R. *Int. J. Nanomedicine* **2010**, *5* (1), 783.

(16) Blower, P. J.; Lewis, J. S.; Zweit, J. *Nucl. Med. Biol.* **1996**, *23* (8), 957.

(17) Anderson, C. J.; Connett, J. M.; Schwarz, S. W.; Rocque, P. a; Guo, L. W.; Philpott, G. W.; Zinn, K. R.; Meares, C. F.; Welch, M. J. *J. Nucl. Med.* **1992**, *33* (9), 1685.

(18) Mastren, T.; Pen, A.; Peaslee, G. F.; Wozniak, N.; Loveless, S.; Essenmacher, S.; Sobotka, L. G.; Morrissey, D. J.; Lapi, S. E. *Sci. Rep.* **2014**, *4*, 6706.

(19) Wadas, T.; Wong, E.; Weisman, G.; Anderson, C. *Curr. Pharm. Des.* **2007**, *13* (1), 3.

(20) Shokeen, M.; Anderson, C. J. *Acc. Chem. Res.* **2009**, *42* (7), 832.

(21) Persson, I. *Pure Appl. Chem.* **2010**, *82* (10), 1901.

(22) Brechbiel, M. W. *Q. J. Nucl. Med. Mol. Imaging* **2008**, *46* (1), 1.

(23) Holland, J. P.; Aigbirhio, F. I.; Betts, H. M.; Bonnitcha, P. D.; Burke, P.; Christlieb, M.; Churchill, G. C.; Cowley, A. R.; Dilworth, J. R.; Donnelly, P. S.; Green, J. C.; Peach, J. M.; Vasudevan, S. R.; Warren, J. E. *Inorg. Chem.* **2007**, *46* (2), 465.

(24) Philpott, G. W.; Schwarz, S. W.; Anderson, C. J.; Dehdashti, F.; Connett, J. M.; Zinn, K. R.; Meares, C. F.; Cutler, P. D.; Welch, M. J.; Siegel, B. a. *J. Nucl. Med.* **1995**, *36* (10), 1818.

(25) Philpott, G. W.; Siegel, B. A.; Schwarz, S. W.; Connett, J. M.; Rocque, P. A.; Fleshman, J. W.; Wallis, J. W.; Baumann, M.; Sun, Y.; Martell, A. E.; Welch, M. J. *Dis. Colon Rectum* **1994**, *37* (8), 782.

(26) Connett, J. M.; Anderson, C. J.; Guo, L. W.; Schwarz, S. W.; Zinn, K. R.; Rogers, B. E.; Siegel, B. A.; Philpott, G. W.; Welch, M. J. *Proc. Natl. Acad. Sci. U. S. A.* **1996**, *93* (13), 6814.

(27) Kukis, D. L.; DeNardo, G. L.; DeNardo, S. J.; Mirick, G. R.; Miers, L. A.; Greiner, D. P.;

Meares, C. F. *Cancer Res.* **1995**, *55* (4), 878.

(28) O'Donnell, R. T.; DeNardo, G. L.; Kukis, D. L.; Lamborn, K. R.; Shen, S.; Yuan, A. N.; Goldstein, D. S.; Carr, C. E.; Mirick, G. R.; DeNardo, S. J. *J. Nucl. Med.* **1999**, *40* (12), 2014.

(29) DeNardo, S. J.; DeNardo, G. L.; Kukis, D. L.; Shen, S.; Kroger, L. a; DeNardo, D. a; Goldstein, D. S.; Mirick, G. R.; Salako, Q.; Mausner, L. F.; Srivastava, S. C.; Meares, C. F. *J. Nucl. Med.* **1999**, *40* (2), 302.

(30) Lewis, M. R.; Boswell, C. a; Laforest, R.; Buettner, T. L.; Ye, D.; Connett, J. M.; Anderson, C. J. *Cancer Biother. Radiopharm.* **2001**, *16* (6), 483.

(31) Kukis, D. L.; Diril, H.; Greiner, D. P.; Denardo, S. J.; Denardo, G. L.; Salako, Q. A.; Meares, C. F. *Cancer* **1994**, *73* (3 S), 779.

(32) Tamura, K.; Kurihara, H.; Yonemori, K.; Tsuda, H.; Suzuki, J.; Kono, Y.; Honda, N.; Kodaira, M.; Yamamoto, H.; Yunokawa, M.; Shimizu, C.; Hasegawa, K.; Kanayama, Y.; Nozaki, S.; Kinoshita, T.; Wada, Y.; Tazawa, S.; Takahashi, K.; Watanabe, Y.; Fujiwara, Y. *J. Nucl. Med.* **2013**, *54* (11), 1869.

(33) Mortimer, J. E.; Bading, J. R.; Park, J. M.; Frankel, P. H.; Carroll, M. I.; Tran, T. T.; Poku, E. K.; Rockne, R. C.; Raubitschek, A. A.; Shively, J. E.; Colcher, D. M. *J. Nucl. Med.* **2017**, No. 626, jnumed.117.193888.

(34) Kurihara, H.; Hamada, A.; Yoshida, M.; Shimma, S.; Hashimoto, J.; Yonemori, K.; Tani, H.; Miyakita, Y.; Kanayama, Y.; Wada, Y.; Kodaira, M.; Yunokawa, M.; Yamamoto, H.; Shimizu, C.; Takahashi, K.; Watanabe, Y.; Fujiwara, Y.; Tamura, K. *EJNMMI Res.* **2015**, *5*, 8.

(35) Ping Li, W.; Meyer, L. A.; Capretto, D. A.; Sherman, C. D.; Anderson, C. J. *Cancer*

Biother. Radiopharm. **2008**, *23* (2), 158.

(36) Niu, G.; Sun, X.; Cao, Q.; Courter, D.; Koong, A.; Le, Q.-T.; Gambhir, S. S.; Chen, X. *Clin. Cancer Res.* **2010**, *16* (7), 2095.

(37) Zeng, D.; Guo, Y.; White, A. G.; Cai, Z.; Modi, J.; Ferdani, R.; Anderson, C. J. *Mol. Pharm.* **2014**, *11* (11), 3980.

(38) Holland, J. P.; Sheh, Y.; Lewis, J. S. *Nucl. Med. Biol.* **2009**, *36* (7), 729.

(39) Kobayashi, T.; Sasaki, T.; Takagi, I.; Moriyama, H. *J. Nucl. Sci. Technol.* **2007**, *44* (February 2014), 90.

(40) Schwarzenbach, G.; Schwarzenbach, K. *Helv. Chim. Acta* **1963**, *22* (1902), 1390.

(41) Holland, J. P.; Divilov, V.; Bander, N. H.; Smith-Jones, P. M.; Larson, S. M.; Lewis, J. S. *J. Nucl. Med.* **2010**, *51* (8), 1293.

(42) Holland, J. P.; Vasdev, N. *Dalt. Trans.* **2014**, *43* (26), 9872.

(43) Holland, J. P.; Caldas-Lopes, E.; Divilov, V.; Longo, V. a; Taldone, T.; Zatorska, D.; Chiosis, G.; Lewis, J. S. *PLoS One* **2010**, *5* (1), e8859.

(44) Rylova, S. N.; Del Pozzo, L.; Klingeberg, C.; Tonnesmann, R.; Illert, A. L.; Meyer, P. T.; Maecke, H. R.; Holland, J. P. *J Nucl Med* **2016**, *57* (1), 96.

(45) Heneweer, C.; Holland, J. P.; Divilov, V.; Carlin, S.; Lewis, J. S. *J. Nucl. Med.* **2011**, *52* (4), 625.

(46) Abou, D. S.; Ku, T.; Smith-Jones, P. M. *Nucl. Med. Biol.* **2011**, *38* (5), 675.

(47) Heskamp, S.; Raavé, R.; Boerman, O. C.; Rijpkema, M.; Goncalves, V.; Denat, F. *Bioconjug. Chem.* **2017**, acs. bioconjchem.7b00325.

(48) Deri, M. A.; Ponnala, S.; Kozlowski, P.; Burton-Pye, B. P.; Cicek, H. T.; Hu, C.; Lewis, J. S.; Francesconi, L. C. *Bioconjug. Chem.* **2015**, *26* (12), 2579.

(49) Deri, M. A.; Ponnala, S.; Zeglis, B. M.; Pohl, G.; Dannenberg, J. J.; Lewis, J. S.; Francesconi, L. C. *J. Med. Chem.* **2014**, *57* (11), 4849.

(50) Tinianow, J. N.; Pandya, D. N.; Pailloux, S. L.; Ogasawara, A.; Vanderbilt, A. N.; Gill, H. S.; Williams, S. P.; Wadas, T. J.; Magda, D.; Marik, J. *Theranostics* **2016**, *6* (4), 511.

(51) Patra, M.; Bauman, A.; Mari, C.; Fischer, C. A.; Blacque, O.; Häussinger, D.; Gasser, G.; Mindt, T. L. *Chem. Commun.* **2014**, *50* (78), 11523.

(52) Ma, M. T.; Meszaros, L. K.; Paterson, B. M.; Berry, D. J.; Cooper, M. S.; Ma, Y.; Hider, R. C.; Blower, P. J. *Dalt. Trans.* **2015**, *44* (11), 4884.

(53) Boros, E.; Holland, J. P.; Kenton, N.; Rotile, N.; Caravan, P. *Chempluschem* **2016**, *81* (3), 274.

(54) Schwertmann, U. *Plant Soil* **1991**, *130*, 1.

(55) Vosjan, M. J. W. D.; Perk, L. R.; Visser, G. W. M.; Budde, M.; Jurek, P.; Kiefer, G. E.; van Dongen, G. A. M. S. *Nat. Protoc.* **2010**, *5* (4), 739.

(56) Pandit-Taskar, N.; O'Donoghue, J. A.; Beylergil, V.; Lyashchenko, S.; Ruan, S.; Solomon, S. B.; Durack, J. C.; Carrasquillo, J. A.; Lefkowitz, R. A.; Gonen, M.; Lewis, J. S.; Holland, J. P.; Cheal, S. M.; Reuter, V. E.; Osborne, J. R.; Loda, M. F.; Smith-Jones, P. M.; Weber, W. A.; Bander, N. H.; Scher, H. I.; Morris, M. J.; Larson, S. M. *European Journal of Nuclear Medicine and Molecular Imaging*. 2014, pp 2093–2105.

(57) Morris, M. J.; Pandit-Taskar, N.; Carrasquillo, J. A.; O'Donoghue, J. A.; Humm, J.; Lyashchenko, S. K.; Haupt, E. C.; Bander, N. H.; Tagawa, S. T.; Holland, J. P.; Smith-Jones, P. M.; Lewis, J. S.; Solomon, S. B.; Scher, H. I.; Larson, S. M. *J. Clin. Oncol.* **2013**, *31* (6).

(58) Pandit-Taskar, N.; O'Donoghue, J. A.; Durack, J. C.; Lyashchenko, S. K.; Cheal, S. M.;

Beylergil, V.; Lefkowitz, R. A.; Carrasquillo, J. A.; Martinez, D. F.; Fung, A. M.; Solomon, S. B.; Gönen, M.; Heller, G.; Loda, M.; Nanus, D. M.; Tagawa, S. T.; Feldman, J. L.; Osborne, J. R.; Lewis, J. S.; Reuter, V. E.; Weber, W. A.; Bander, N. H.; Scher, H. I.; Larson, S. M.; Morris, M. J. *Clin. Cancer Res.* **2015**, *21* (23), 5277.

(59) Koizumi, M.; Endo, K.; Kunimatsu, M.; Sakahara, H.; Nakashima, T.; Kawamura, Y.; Watanabe, Y.; Saga, T.; Konishi, J.; Yamamuro, T.; Hosoi, S.; Toyama, S.; Arano, Y.; Yokoyama, A. *Cancer Res.* **1988**, *48* (5), 1189.

(60) Govindan, S. V.; Michel, R. B.; Griffiths, G. L.; Goldenberg, D. M.; Mattes, M. J. *Nucl. Med. Biol.* **2005**, *32* (5), 513.

(61) Othman, M. F. bin; Mitry, N. R.; Lewington, V. J.; Blower, P. J.; Terry, S. Y. A. *Nucl. Med. Biol.* **2017**, *46*, 12.

(62) Ryan, K. P.; Dillman, R. O.; DeNardo, S. J.; DeNardo, G. L.; Beauregard, J.; Hagan, P. L.; Amox, D. G.; Clutter, M. L.; Burnett, K. G.; Rulot, C. M. *Radiology* **1988**, *167* (1), 71.

(63) Alberto, R.; Braband, H. *SPECT/PET Imaging with Technetium, Gallium, Copper, and Other Metallic Radionuclides*; Elsevier Ltd., 2013; Vol. 3.

(64) Quigley, A. M.; Gnanasegaran, G.; Buscombe, J. R.; Hilson, A. J. W. *Med. Princ. Pract.* **2008**, *17* (6), 447.

(65) Adam, M. J.; Wilbur, D. S. *Chem. Soc. Rev.* **2005**, *34* (2), 153.

(66) Watkinson, J. C.; Maisey, M. N. *J. R. Soc. Med.* **1988**, *81* (11), 653.

(67) Hamill, T. G.; Duggan, M. E.; Perkins, J. J. *J. Label. Comp. Radiopharm.* **2001**, *44* (1), 55.

(68) Pentlow, K. S.; Graham, M. C.; Lambrecht, R. M.; Daghighian, F. *J. Nucl. Med.* **1996**, *37* (9), 1557.

(69) McConahey, P. J.; Dixon, F. J. *Int. Arch. Allergy. Immunol.* **1966**, *29* (2), 185.

(70) Markwell, M. A. K. *Anal. Biochem.* **1982**, *125* (2), 427.

(71) Salacinski, P. R. P.; McLean, C.; Sykes, J. E. C.; Clement-Jones, V. V; Lowry, P. J. *Anal. Biochem.* **1981**, *117* (1), 136.

(72) Wilbur, D. S. *Bioconjugate Chem.* **1992**, *3* (6), 433.

(73) Kaminski, M. S.; Tuck, M.; Estes, J.; Kolstad, A.; Ross, C. W.; Zasadny, K.; Regan, D.; Kison, P.; Fisher, S.; Kroll, S. *New Engl. J. Med.* **2005**, *352* (5), 441.

(74) Press, O. W.; Eary, J. F.; Gooley, T.; Gopal, A. K.; Liu, S.; Rajendran, J. G.; Maloney, D. G.; Petersdorf, S.; Bush, S. A.; Durack, L. D. *Blood* **2000**, *96* (9), 2934.

(75) Lebovic, D.; Kaminski, M. S.; Anderson, T. B.; Detweiler-Short, K.; Griffith, K. A.; Jobkar, T. L.; Kandarpa, M.; Jakubowiak, A. Am. Soc. Hematology 2012,.

(76) DeNardo, G. L.; DeNardo, S. J.; Goldstein, D. S.; Kroger, L. A.; Lamborn, K. R.; Levy, N. B.; McGahan, J. P.; Salako, Q.; Shen, S.; Lewis, J. P. *J. Clin. Oncol.* **1998**, *16* (10), 3246.

(77) Shapiro, W. R.; Carpenter, S. P.; Roberts, K.; Shan, J. S. *Expert Opin. Biol. Ther.* **2006**, *6* (5), 539.

(78) Hdeib, A.; Sloan, A. E. *Expert Opin. Biol. Ther.* **2011**, *11* (6), 799.

(79) Chen, S.; Yu, L.; Jiang, C.; Zhao, Y.; Sun, D.; Li, S.; Liao, G.; Chen, Y.; Fu, Q.; Tao, Q. *J. Clin. Oncol.* **2005**, *23* (7), 1538.

(80) Braghirolli, A. M. S.; Waissmann, W.; da Silva, J. B.; dos Santos, G. R. *Appl. Radiat. Isot.* **2014**, *90*, 138.

(81) Verel, I.; Visser, G. W. M.; Vosjan, M. J. W. D.; Finn, R.; Boellaard, R.; van Dongen, G. A. M. S. *Eur. J. Nucl. Med. Mol. Imaging* **2004**, *31* (12), 1645.

(82) Tijink, B. M.; Perk, L. R.; Budde, M.; Stigter-van Walsum, M.; Visser, G. W. M.; Kloet, R. W.; Dinkelborg, L. M.; Leemans, C. R.; Neri, D.; van Dongen, G. A. M. S. *Eur. J. Nucl. Med. Mol. Imaging* **2009**, *36* (8), 1235.

(83) Wadas, T. J.; Wong, E. H.; Weisman, G. R.; Anderson, C. J. *Chem. Rev.* **2010**, *110* (5), 2858.

(84) Chinol, M.; Hnatowich, D. J. *J. Nucl. Med.* **1987**, *28* (9), 1465.

(85) Herzog, H.; Tellmann, L.; Scholten, B.; Coenen, H. H.; Qaim, S. M. *Q. J. Nucl. Med. Mol. Imaging* **2008**, *52* (2), 159.

(86) Parr, R. G.; Pearson, R. G. *J. Am. Chem. Soc.* **1983**, *105* (26), 7512.

(87) Jang, Y. H.; Blanco, M.; Dasgupta, S.; Keire, D. A.; Shively, J. E.; Goddard, W. A. *J. Am. Chem. Soc.* **1999**, *121* (26), 6142.

(88) Stimmel, J. B.; Stockstill, M. E.; Kull Jr, F. C. *Bioconjugate Chem.* **1995**, *6* (2), 219.

(89) Kobayashi, H.; Wu, C.; Yoo, T. M.; Bao-Fu, S. *J. Nucl. Med.* **1998**, *39* (5), 829.

(90) Kang, C. S.; Sun, X.; Jia, F.; Song, H. A.; Chen, Y.; Lewis, M.; Chong, H.-S. *Bioconjugate Chem.* **2012**, *23* (9), 1775.

(91) Price, E. W.; Edwards, K. J.; Carnazza, K. E.; Carlin, S. D.; Zeglis, B. M.; Adam, M. J.; Orvig, C.; Lewis, J. S. *Nucl. Med. Biol* **2016**, *43* (9), 566.

(92) Witzig, T. E.; Gordon, L. I.; Cabanillas, F.; Czuczman, M. S.; Emmanouilides, C.; Joyce, R.; Pohlman, B. L.; Bartlett, N. L.; Wiseman, G. A.; Padre, N. *J. Clin. Oncol.* **2002**, *20* (10), 2453.

(93) Thompson, S.; Ballard, B.; Jiang, Z.; Revskaya, E.; Sisay, N.; Miller, W. H.; Cutler, C. S.; Dadachova, E.; Francesconi, L. C. *Nucl. Med. Biol* **2014**, *41* (3), 276.

(94) Kulik, L. M.; Atassi, B.; Van Holsbeeck, L.; Souman, T.; Lewandowski, R. J.; Mulcahy,

M. F.; Hunter, R. D.; Nemcek, A. A.; Abecassis, M. M.; Haines, K. G. *J. Surg. Oncol.* **2006**, *94* (7), 572.

(95) Lindén, O.; Hindorf, C.; Cavallin-Ståhl, E.; Wegener, W. A.; Goldenberg, D. M.; Horne, H.; Ohlsson, T.; Stenberg, L.; Strand, S.-E.; Tennvall, J. *Clin. Can. Res.* **2005**, *11* (14), 5215.

(96) Salako, Q. A.; O'Donnell, R. T.; DeNardo, S. J. *J Nucl Med* **1998**, *39* (4), 667.

(97) Cwikla, J. B.; Sankowski, A.; Seklecka, N.; Buscombe, J. R.; Nasierowska-Guttmejer, A.; Jeziorski, K. G.; Mikolajczak, R.; Pawlak, D.; Stepien, K.; Walecki, J. *Ann. Oncol.* **2009**, *21* (4), 787.

(98) Dvorakova, Z.; Henkelmann, R.; Lin, X.; Türler, A.; Gerstenberg, H. *Appl. Radiat. Isot.* **2008**, *66* (2), 147.

(99) Bilewicz, A.; Żuchowska, K.; Bartoś, B. *J. Radioanal. Nucl. Chem.* **2009**, *280* (1), 167.

(100) Aime, S.; Barge, A.; Botta, M.; Fasano, M.; Ayala, J. D.; Bombieri, G. *Inorg. Chim. Acta* **1996**, *246* (1–2), 423.

(101) Stimmel, J. B.; Kull, F. C. *Nucl. Med. Biol* **1998**, *25* (2), 117.

(102) Price, E. W.; Zeglis, B. M.; Cawthray, J. F.; Ramogida, C. F.; Ramos, N.; Lewis, J. S.; Adam, M. J.; Orvig, C. *J. Am. Chem. Soc.* **2013**, *135* (34), 12707.

(103) Banerjee, S.; Pillai, M. R. A.; Knapp, F. F. *Chem. Rev.* **2015**, *115* (8), 2934.

(104) Strosberg, J.; Wolin, E.; Chasen, B.; Kulke, M.; Bushnell, D.; Caplin, M.; Baum, R. P.; Mittra, E.; Hobday, T.; Hendifar, A. *Eur. J. Cancer* **2015**, *51*, S710.

(105) Frilling, A.; Weber, F.; Saner, F.; Bockisch, A.; Hofmann, M.; Mueller-Brand, J.; Broelsch, C. E. *Surgery* **2006**, *140* (6), 968.

(106) Yong, K.; Brechbiel, M. W. *Dalt. Trans.* **2011**, *40* (23), 6068.

(107) Su, F.-M.; Beaumier, P.; Axworthy, D.; Atcher, R.; Fritzberg, A. *Nucl. Med. Biol.* **2005**, *32* (7), 741.

(108) Atcher, R. W.; Friedman, A. M.; Hines, J. J. *Appl. Radiat. Isot.* **1988**, *39* (4), 283.

(109) Mirzadeh, S.; Kumar, K.; Gansow, O. A. *Radiochim. Acta* **1993**, *60* (1), 1.

(110) Chappell, L. L.; Dadachova, E.; Milenic, D. E.; Garmestani, K.; Wu, C.; Brechbiel, M. W. *Nucl. Med. Biol* **2000**, *27* (1), 93.

(111) Macklis, R. M.; Kinsey, B. M.; Kassis, A. I.; Ferrara, J. L. M.; Atcher, R. W.; Hines, J. J.; Coleman, C. N.; Adelstein, S. J.; Burakoff, S. J. *Science (80-.).* **1988**, *240* (4855), 1024.

(112) Meredith, R. F.; Torgue, J.; Azure, M. T.; Shen, S.; Saddekni, S.; Banaga, E.; Carlise, R.; Bunch, P.; Yoder, D.; Alvarez, R. *Cancer Biother. Radiopharm.* **2014**, *29* (1), 12.

(113) Mirzadeh, S. *Appl. Radiat. Isot.* **1998**, *49* (4), 345.

(114) Kang, C. S.; Song, H. A.; Milenic, D. E.; Baidoo, K. E.; Brechbiel, M. W.; Chong, H.-S. *Nucl. Med. Biol* **2013**, *40* (5), 600.

(115) Milenic, D. E.; Roselli, M.; Mirzadeh, S.; Pippin, C. G.; Gansow, O. A.; Colcher, D.; Brechbiel, M. W.; Schlom, J. *Cancer Biother. Radiopharm.* **2001**, *16* (2), 133.

(116) Lima, L. M. P.; Beyler, M.; Oukhatar, F.; Le Saec, P.; Faivre-Chauvet, A.; Platas-Iglesias, C.; Delgado, R.; Tripier, R. *Chem. Commun.* **2014**, *50* (82), 12371.

(117) Lima, L. M. P.; Beyler, M.; Delgado, R.; Platas-Iglesias, C.; Tripier, R. *Inorg. Chem.* **2015**, *54* (14), 7045.

(118) McDevitt, M. R.; Barendswaard, E.; Ma, D.; Lai, L.; Curcio, M. J.; Sgouros, G.; Ballangrud, Å. M.; Yang, W.-H.; Finn, R. D.; Pellegrini, V. *Cancer Res.* **2000**, *60* (21), 6095.

(119) Sgouros, G.; Ballangrud, A. M.; Jurcic, J. G.; McDevitt, M. R. *J. Nucl. Med.* **1999**, *40*

(11), 1935.

(120) Sathekge, M.; Knoesen, O.; Meckel, M.; Modiselle, M.; Vorster, M.; Marx, S. *Eur. J. Nucl. Med. Mol. Imaging* **2017**, *44* (6), 1099.

(121) Kratochwil, C.; Giesel, F. L.; Bruchertseifer, F.; Mier, W.; Apostolidis, C.; Boll, R.; Murphy, K.; Haberkorn, U.; Morgenstern, A. *Eur. J. Nucl. Med. Mol. Imaging* **2014**, *41* (11), 2106.

(122) Apostolidis, C.; Molinet, R.; Rasmussen, G.; Morgenstern, A. *Anal. Chem.* **2005**, *77* (19), 6288.

(123) Apostolidis, C.; Molinet, R.; McGinley, J.; Abbas, K.; Möllenbeck, J.; Morgenstern, A. *Appl. Radiat. Isot.* **2005**, *62* (3), 383.

(124) Ferrier, M. G.; Batista, E. R.; Berg, J. M.; Birnbaum, E. R.; Cross, J. N.; Engle, J. W.; La Pierre, H. S.; Kozimor, S. A.; Pacheco, J. S. L.; Stein, B. W. *Nat. Commun.* **2016**, *7*, 12312.

(125) Ferrier, M. G.; Stein, B. W.; Batista, E. R.; Berg, J. M.; Birnbaum, E. R.; Engle, J. W.; John, K. D.; Kozimor, S. A.; Lezama Pacheco, J. S.; Redman, L. N. *ACS Cent. Sci.* **2017**, *3* (3), 176.

(126) Deal, K. A.; Davis, I. A.; Mirzadeh, S.; Kennel, S. J.; Brechbiel, M. W. *J. Med. Chem.* **1999**, *42* (15), 2988.

(127) Thiele, N. A.; Brown, V.; Kelly, J. M.; Amor-Coarasa, A.; Jermilova, U.; MacMillan, S. N.; Nikolopoulou, A.; Ponnala, S.; Ramogida, C. F.; Robertson, A. K. H. *Angew. Chem. Int. Ed.* **2017**, *accepted*.

(128) Ravandi, F.; Pagel, J. M.; Park, J. H.; Douer, D.; Estey, E. H.; Kantarjian, H. M.; Cicic, D.; Scheinberg, D. A. Am. Soc. Hematol. 2013,.

Figure 1. Stacked bar chart showing the total number of US-FDA approved New Molecular Entities from 2011 until August 2017 with a breakdown showing the contribution from mAb-based agents and other drugs. * Data available until 08/2017.

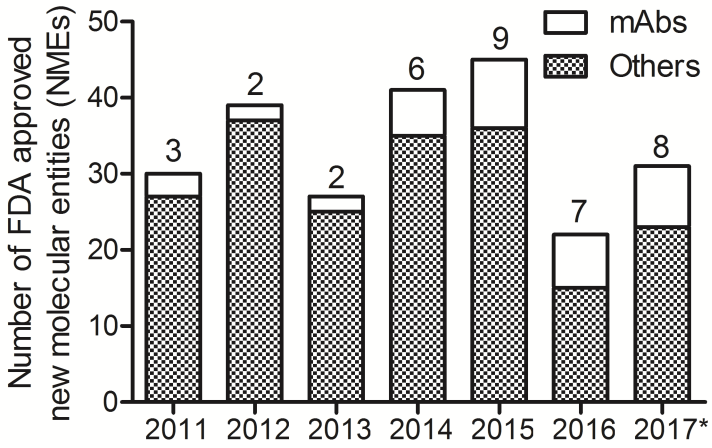

Figure 2. Schematic representation of a radiolabelled mAb involving chemical modification of the protein using covalent bond formation to a radiometal binding chelate *via* a linker group.

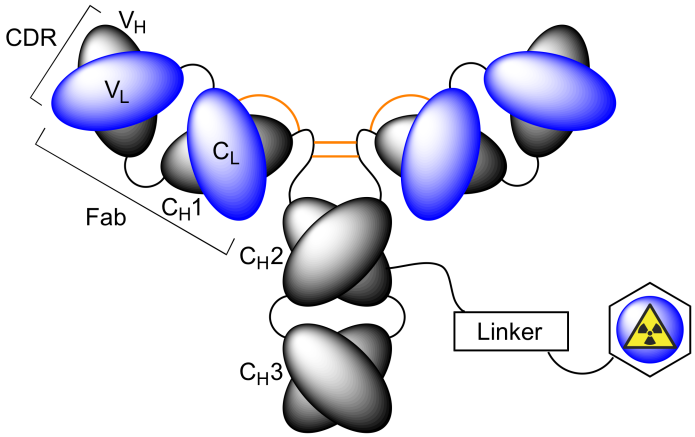

Figure 3. Chemical structures of selected chelates that have been employed for complexation of various radiometal ions including those of copper, gallium, indium, yttrium, lutetium, actinium and beyond.

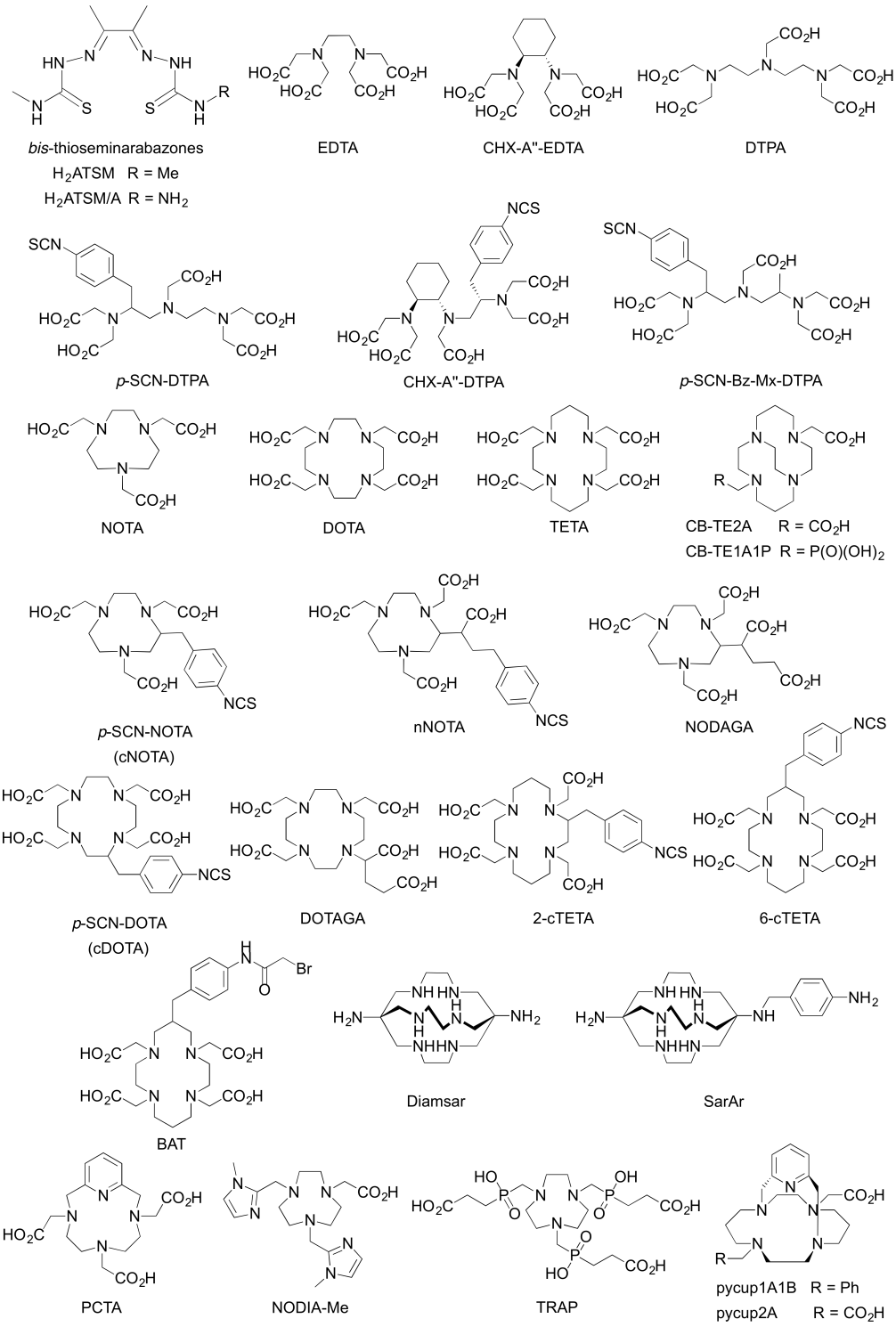

Figure 4. Chemical conjugation of TETA and BAT-2IT to antibodies coupling to the ε-NH_2 group of lysine residues.

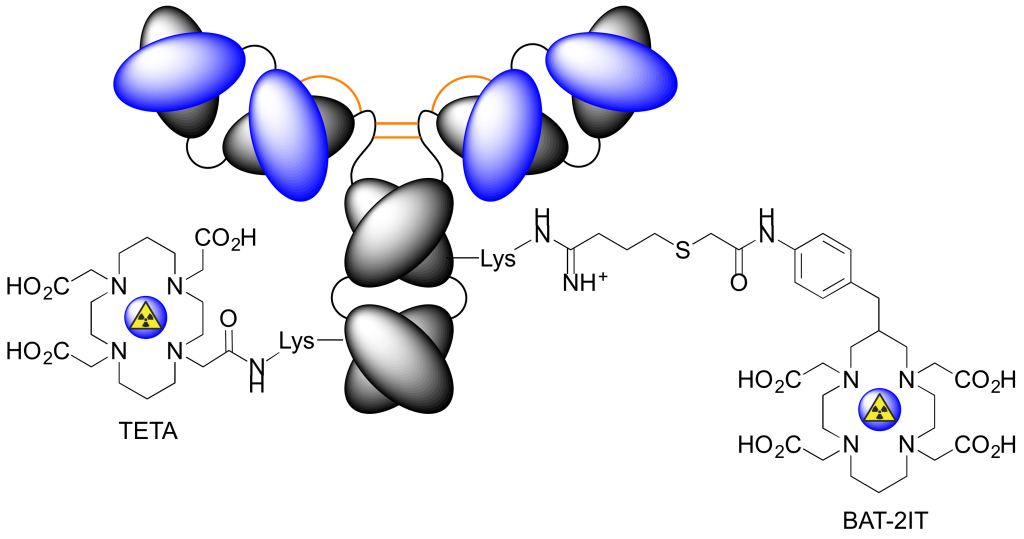

Figure 5. Chemical structures of selected bifunctional chelates that have been developed for derivatisation of proteins and complexation of $^{89}Zr^{4+}$ ions.

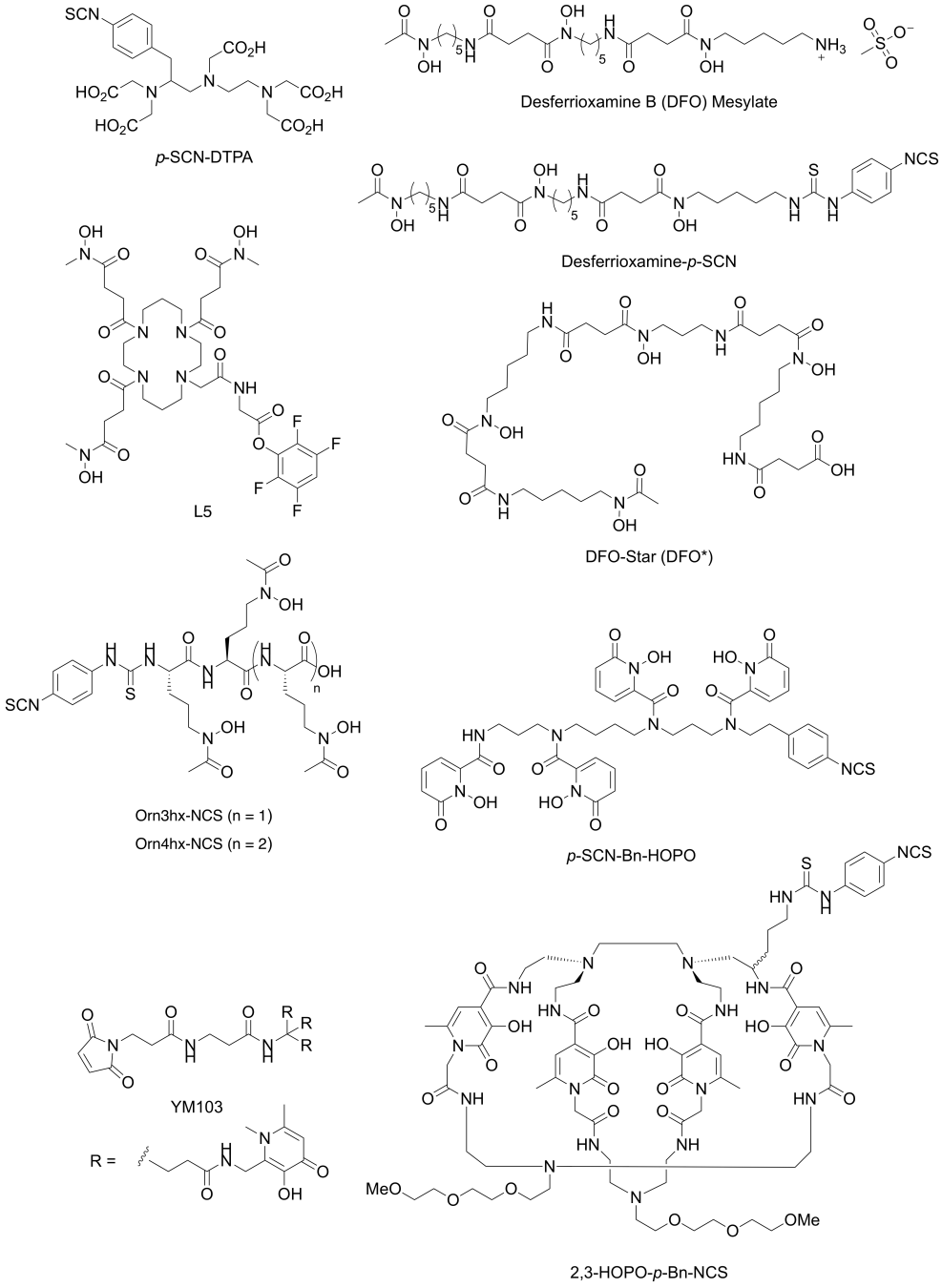

Figure 6. Chemical structures of ^{99m}Tc chelates that incorporate different '^{99m}Tc-cores'.

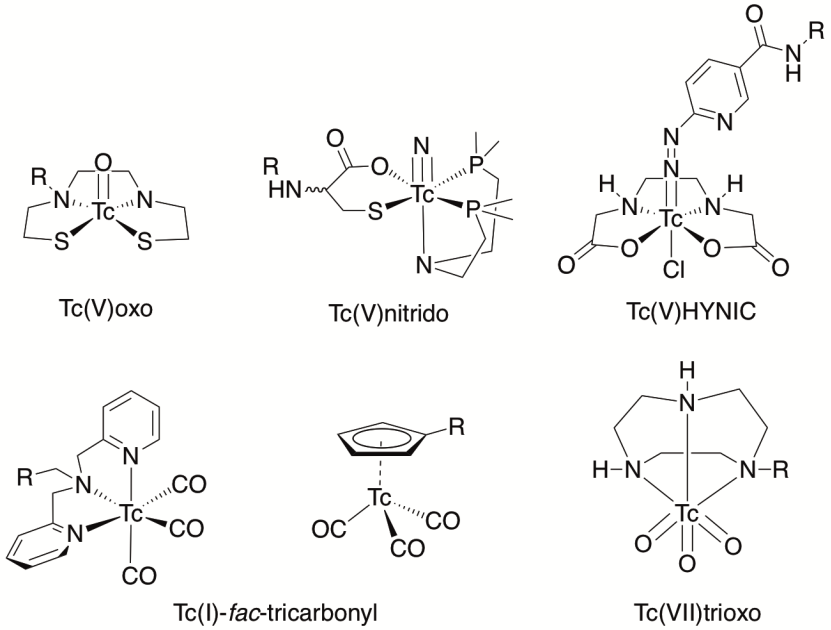

Figure 7. Chemical structures of various reagents used for oxidative radiolabelling of proteins with iodine radionuclides.

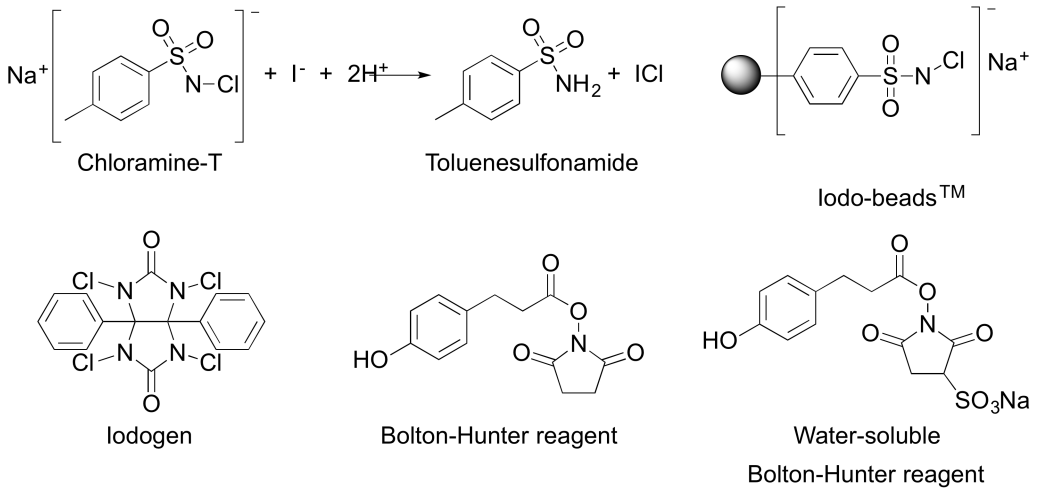

Figure 8. Chemical structures of selected chelates that have been employed for complexation of yttrium, lutetium, bismuth, lead and actinium.

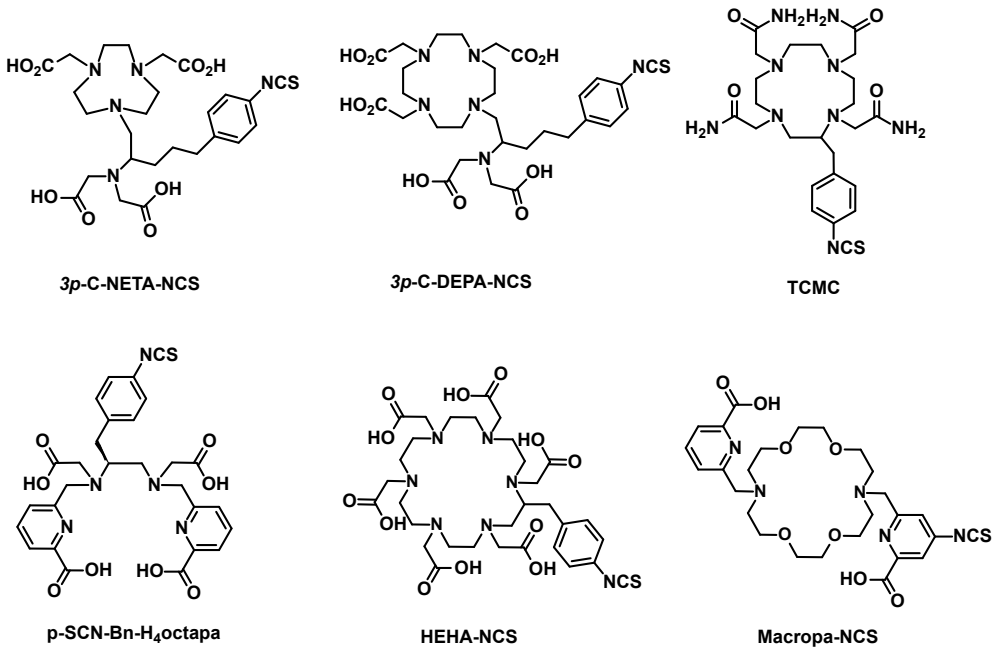

Table 1. Physical decay characteristics of various radionuclides that have potential applications in diagnostic imaging and radioimmunotherapy with antibody-based radiopharmaceuticals.

Radionuclide	Half-life, $t_{1/2}$	Decay mode (% branching ratio)	Production route(s)	GS-GS Q-value (keV)	Particle end-point energy / keV	Application
^{64}Cu	12.701 h	ε+β+ (61.5%) β+ (17.60%) β- (38.5%)	^{64}Ni(p,n)^{64}Cu	1675.03 (^{64}Ni) 579.4 (^{64}Zn)	β+ 653.03 β- 579.4	Immuno-PET and RIT
^{67}Cu	61.83 h	β- (100%)	^{68}Zn(p,2p)^{67}Cu ^{70}Zn(p,α)^{67}Cu ^{67}Zn(n,p)^{67}Cu ^{68}Zn(γ,p)^{67}Cu	561.7	β- 561.7	RIT (Immuno-SPECT)
^{67}Ga	3.2617 d	ε (100%)	^{nat}Zn(p,x)^{67}Ga ^{68}Zn(p,2n)^{67}Ga	1000.8	Auger and CE	Immuno-SPECT and RIT
^{86}Y	14.74 h	ε+β+ (100%) β+ (31.9%)	^{86}Sr(p,n)^{86}Y	5240	β+ 3141	Immuno-PET
^{89}Zr	78.41 h	ε+β+ (100%) β+ (22.74%)	^{89}Y(p,n)^{89}Zr	2833	β+ 902	Immuno-PET
^{90}Y	64.00 h	β- (100%)	^{90}Sr/^{90}Y	2280.1	β- 2280.1	RIT
^{99m}Tc	6.01 h	β- (0.0037%) IT (99.9963%)	^{99}Mo/^{99m}Tc	Excited state (parent) level: 142.68	β- 435.9	Immuno-SPECT
^{111}In	2.8047 d	ε (100%)	^{111}Cd(p,n)^{111m,g}In ^{112}Cd(p,2n)^{111m,g}In	862	Auger and CE	Immuno-SPECT and RIT
^{123}I	13.2234 h	ε (100%)	^{124}Xe(p,2n)^{123}Cs/^{123}Xe/^{123}I ^{124}Xe (p,pn)^{123}I ^{123}Te(p,n)^{123}I	1228.6	Auger and CE	RIT (Immuno-SPECT)
^{124}I	4.1760 d	ε+β+ (100%) β+ (22.7%)	^{124}Te(p,n)^{124}I	3159.6	β+ 2137.6	Immuno-PET
^{131}I	8.0252 d	β- (100%)	^{130}Te(n,γ)^{131}Te/^{131}I	970.8	β- 806.9 Auger and CE	RIT
^{177}Lu	6.647 d	β- (100%)	^{176}Lu(n,γ)^{177}Lu ^{176}Yb(n,γ)^{177}Yb/^{177}Lu	498.3	β- 498.3 Auger and CE	RIT (Immuno-SPECT)
^{213}Bi	45.59 m	α(2.20%) β-(97.80%)	^{225}Ac/^{213}Bi	β- 1423 α 5988	β- 1423 α 5875 Auger and CE	RIT
^{225}Ac	10.0 d	α(100%)	^{229}Th/^{225}Ra/^{225}Ac	5935.1	α 5830 Auger and CE	RIT